TÉCNICO LISBOA

Microwave-assisted synthesis of stable SBA-15 mesoporous supports for CaO-based sorbents suitable for CO_2 capture

Ana Pascual Calavia

Dissertação para obtenção do Grau de Mestre em

Engenharia Química

Orientadores: Prof. Doutora Carla Isabel Costa Pinheiro, (IST/UL)

Doutor Auguste Rodrigues Fernandes, (IST/UL)

Júri

Presidente: Prof. Doutor José Manuel Félix Madeira Lopes, (IST/UL)

Orientador: Prof. Doutora Carla Isabel Costa Pinheiro, (IST/UL)

Vogal: Prof. Doutora Inês Alexandra Morgado do Nascimento Matos, (FCT/UNL)

Julho 2014

AGRADECIMIENTOS

Esta “dissertação” es el resultado de un intenso trabajo, dedicación y esfuerzo, tanto por mi parte como por la de todas las personas que me han ido ayudando durante todo este trayecto.

En primer lugar, quiero agradecer a mi profesora Carla Pinheiro por haberme dado la oportunidad de formar parte de su equipo de trabajo en el Instituto Superior Técnico de Lisboa, que junto con mi orientador Auguste Rodrigues, me han ayudado en todo momento para poder seguir adelante, sobre todo en la recta final del trabajo. Muchas gracias a los dos por dedicarme vuestro tiempo, por conseguir que este proyecto quedara lo mejor posible y por ayudarme a descubrir dónde estaba el "maldito" óxido de calcio. Por esto y por tener tanta paciencia con mi "portuñol" os estaré tremendamente agradecida siempre.

Agradecer también a todo el equipo de trabajo del departamento CRERG (Catalysis and Reaction Engineering Research Group), que desde el primer momento que pusimos un pie dentro, nos recibieron de la mejor manera posible. Gracias por ayudarme siempre que lo he necesitado y muchas más gracias por hacer que todas las horas que hemos pasado trabajando merecieran la pena, por no hablar de la inmensa cantidad de "bolos" que hemos comido.

Quiero agradecer en especial a mis "fofinhas" Liliana, Carminha y Suse. No hace falta poner las razones, ellas saben todo.

Gracias también a toda mi "familia" de Lisboa, esa maravillosa gente que he tenido el placer de conocer aquí y espero que por mucho más tiempo. A pesar de tener que decir casi siempre "no puedo" a todos los planes propuestos entre semana, nunca han dejado de contar conmigo para nada. Espero encantada esa quedada Erasmus en Murcia.

No podía olvidarme de Roberto, mi compañero de batallas tanto fuera del IST como dentro. Nunca olvidaré nuestra primera semana en Lisboa, alimentándonos a base de bocadillos y pateando la ciudad sin parar de llover, hasta que al fin encontramos nuestra casa.

Por último, quería agradecer a las personas más importantes de todas, a mi familia. Este trabajo va dedicado a vosotros, porque habéis estado siempre apoyándome (durante la universidad y en Lisboa). Nunca dejasteis de animarme para irme de Erasmus, aun sabiendo que al final yo no tenía ni una gana de irme de casa. Gracias por todo, por estar siempre ahí. Y en especial, quería dedicar este trabajo a mi padre, que por circunstancias de la vida no ha podido vivir este momento tan importante junto a mí, pero sé que estarás igualmente orgulloso de tu hija pequeña.

Muchas gracias a Lisboa, ha conseguido que me enamore de una ciudad.

MUITO OBRIGADA A TODOS!

ABSTRACT

Nowadays, global warming is turning into a serious problem in the world. Several technologies are been developed with the purpose of decreasing greenhouse gases emissions, mainly CO_2. "Calcium-looping cycle" post-combustion process is an emerging technology using natural or synthetic CaO-sorbents for CO_2 capture. On the other hand, mesoporous materials have been referred to as suitable materials for supporting various metal oxides species in heterogeneous catalysis and adsorption applications, due to their great thermal stability, large surface areas and high pore volume, making them good candidates to support CaO species for CO_2 capture purpose.

This study is focused on the microwave-assisted synthesis of SBA-15 materials and the optimization of the experimental conditions (crystallization time and temperature) to achieve a stable support for CaO-sorbents suitable for CO_2 capture. Calcium was introduced by incipient wetness impregnation, giving two SBA-15 samples with 10 wt-% and 20 wt-% Ca loading. The final Ca-based SBA-15 sorbents were characterized using thermogravimetric analysis (TGA-DSC), X-Ray diffraction (XRD), nitrogen sorption measurements and tested in the carbonation-calcination cycles (lab-scale uint and TG).

Three synthetic non-supported CaO sorbents were also prepared by sol-gel method and the help of structurants and also studied in CO_2 capture process, being the influence of the final calcination temperature and the nature of the carbon matrixes used evaluated.

The results showed that Ca-based SBA-15 samples were not efficient enough in CO_2 capture, due to the very low amount of Ca impregnated in the final materials, although they possessed an ordered mesoporous structure, being necessary to increase the amount of calcium to obtain satisfactory results in CO_2 capture processes.

Concerning the synthetic non-supported sorbents, activated carbon was shown to be the best structurant, in terms of initial reactivity and reactivity decay. The calcination temperature was also shown to be crucial, as a lower temperature let a better initial reactivity.

Key words: Hexagonal SBA-15, mesoporous, microwave, CO_2 capture, calcium oxide, thermal stability.

RESUMO

Actualmente, o aquecimento global é considerado um dos assuntos mais preocupantes no mundo. Foram desenvolvidas diversas tecnologias com o objectivo de diminuir as emissões de gases com efeito de estufa, principalmente o CO_2. Os processos de pós-combustão "*Calcium-looping cycle*" constituem uma tecnologia emergente que usa CaO sintético e/ou natural para a captura de CO_2. Por outro lado, os mesoporosos têm sido referidos como bons suportes para metais em aplicações catalíticas devido à uma elevada estabilidade térmica, elevada área de superfície e elevado volume poroso, entre outras. Por essa razão, estes materiais tornam-se bons candidatos para a preparação de sorventes sintéticos a base de CaO.

Este estudo centrou-se na síntese de SBA-15 através do uso de microondas, variando as condições experimentais de forma a obter suportes estáveis para o CaO aplicáveis nos processos de captura de CO_2, optimizando a temperatura e o tempo de tratamento hidrotérmico. A seguir, foram introduzidas por impregnação a seco quantidades de 10% e 20% em massa de CaO em amostras de SBA-15 que foram posteriormente testadas em ciclos de carbonatação-calcinação (unidade laboratorial e TG). Todas as amostras preparadas foram caracterizadas por diversas técnicas, nomeadamente análise termogravimetrica (TGA), difracção de raios X (XRD) e adsorção-desorção de azoto a 77 K.

Três sorventes sintéticos não suportados foram também preparados, utilizando o método sol-gel e carvões desempenhendo o papel de estruturante. A influência da temperatura final de calcinação bem com a natureza do estruturante utilizado foram analisados.

Os resultados mostraram que as amostras SBA-15 preparadas com Ca não demonstraram uma grande eficiência na captura de CO_2, devido à baixa quantidade de cálcio impregnado, embora os materiais finais apresentarem a estrutura mesoporosa original. Par obter resultados satisfatórios, seria importante aumentar drasticamente o teor de Ca nas amostras finais.

No que diz respeito aos sorventes sintéticos não suportados, o carvao activado tem sido a melhora escolha, demonstrado uma boa reactividade inicial que permanece constante ao longo do tempo. A temperatura de calcinaçao também demonstrou ser um parámetro fundamental, uma temperatura menor permitindo obter uma reactividade inicial maior.

Palavras chave: SBA-15 hexagonal, mesoporosos, microondas, captura de CO_2, óxido de cálcio, estabilidade térmica.

TABLE OF CONTENTS

LIST OF FIGURES

LIST OF TABLES

LIST OF ABBREVIATIONS

TGA: Thermogravimetric Analysis

DSC: Differential Scanning Calorimetric

XRD: X-Ray Diffraction

CCS: Carbon Capture and Storage

SBA-15: Santa Barbara Amorphous-15

MCM-41: Mobil Composition of Matter No. 41

IPPC: Intergovernmental Panel on Climate Change

IEA: International Energy Agency

PCC: Precipitated Calcium Carbonate

IUPAC: International Union of Pure and Applied Chemistry

MARS-5: Microwave-Accelerated Reaction System

BJH: Barett-Joyner-Halenda

BET: Brunauer, Emmett and Teller Model

BP2000: Black Pearl 2000

ASAP: Accelerated Surface Area and Porosimetry Analyser

1 INTRODUCTION

Due to the large growth of the use of technology in the society, industries have been increasing the energy consumption with the consequent increase in the burning of fossil fuels for energy production. This has produced a greater emission of gases into the atmosphere, causing the greenhouse effect, mainly CO_2. Nowadays, the demand for mitigation of these emissions is widely accepted. Carbon Capture and Storage (CCS) technologies aim to capture and provide suitable streams for appropriate storage, mitigating the CO_2 emissions.

For the sequestration step of CO_2, different sorbents are used: naturals or synthetics. Recently, calcium oxide is the most used due to its low price and widely availability. Ca-based sorbents are used in the "calcium looping cycles" and have a large adsorption capacity at high temperatures. The major challenge in these cycles is the deactivation suffered by the sorbents, for that reason many methods have been proposed for reducing that effect and improving the adsorption capacity. Many researchers are studying the modification of the pore structure as a solution for enhancing the stability of sorbents.

The discovery of mesoporous silica materials, mainly SBA-15 in 1998, was a significant progress and has achieved considerable attention in recent years due to their high surface area, large pore volume and effectiveness as a sorbents. Synthesis of SBA-15 is composed by two principal steps: ripening and aging. Different routes have been developed in the synthesis in order to improve the hydrothermal stability of SBA-15 and to reduce of time, energy and cost without decrease the quality of the mesoporous material. The microwave-assisted synthesis in the hydrothermal step have resulted a successfully method, supplying a shorter crystallization time compared with the conventional method.

Therefore, this work is focused in the synthesis and stability study of SBA-15 at high temperatures under microwave conditions with the purpose of use the mesoporous material as support of CaO, improving the uptake capacity of synthetic sorbents in calcium-looping cycles processes. Nowadays, there are not many studies about the use of SBA-15 as support of CaO for CO_2 capture.

The report is divided in six sections. Chapter 1 describes the part of literature review, explaining in detail all items presented above. Secondly, the different materials and methods used in the synthesis and characterization of samples are explained. Chapter 3 is dedicated to the description of the adsorption lab-scale unit along with the experimental method necessary. In chapter 4, all experimental results are presented. Chapter 5 and 6 are reserved for final conclusions and future work, respectively.

2 LITERATURE REVIEW

2.1 Global warming problem

One of the most important concern in the world is the global warming, being the principle cause the increasing dependence on the combustion of fossil fuels to produce energy (coal, petroleum and natural gas). This reason and others human activities (deforestation, industrial processes or some agricultural practises) are the most responsible causes for gases emissions into atmosphere, causing the so-called "greenhouse effect".
The principle greenhouse gases emitted are (1):

- **Carbon dioxide (CO_2):** the most important sources of CO_2 are the fossil fuel use, chemical processing (for example, cement industries) and the deforestation due to the way in which people use the land. However, land can also remove CO_2 from the atmosphere through reforestation, improvement of soils and other activities.

- **Methane (CH_4):** this gas is emitted in agricultural activities, waste management and energy use.

- **Nitrous oxide (N_2O):** the primary source is the fertilizer use in agricultural activities.

- **Fluorinated gases (F-gases):** industrial processes, refrigeration and the use of a variety of consumer products contribute to emissions of F-gases, including hydrofluorocarbons (HFCs), perfluorocarbons (PFCs) and sulfur hexafluoride (SF6).

The changing concentrations of these greenhouse gases are the major responsible factors to the increase in temperature. The Intergovernmental Panel on Climate Change (IPPC) estimates that, by year 2100, the atmosphere could contain up to 570 ppm of CO_2 , rising the global temperature of around 1.9ºC and increasing the sea level in 3.8 m (2).

Carbon dioxide is the most contributor gas (82%) to the global warming, because of combustion fuels and industrial processes. Emissions have increased approximately 80% between 1970 and 2004 (3). The Commission of the European Communities has stated that for climate change being limited to 2K, emissions in the developed world must be reduced by 30% by 2020, rising to 60-80% by 2050. However, the Commission affirmed that these targets would not be achieved without implementation of any solution (4).

There are three key options for reducing the total CO_2 emissions into the atmosphere (2):

1) reducing energy intensity, which requires efficient use of energy.
2) reducing the carbon intensity using non-fossil fuels such as renewable energies.
3) improving the sequestration of CO_2.

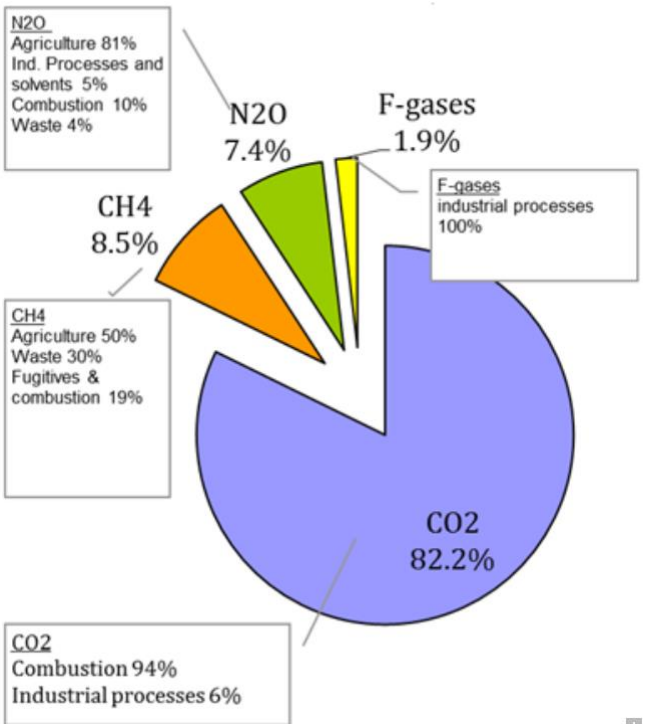

Figure 1: Total greenhouse gas emissions by gas in EU in 2011. (5)

In the next figure, the evolution of CO_2 emissions is shown from 1850 to 2010, including the future emissions projected in the following years.

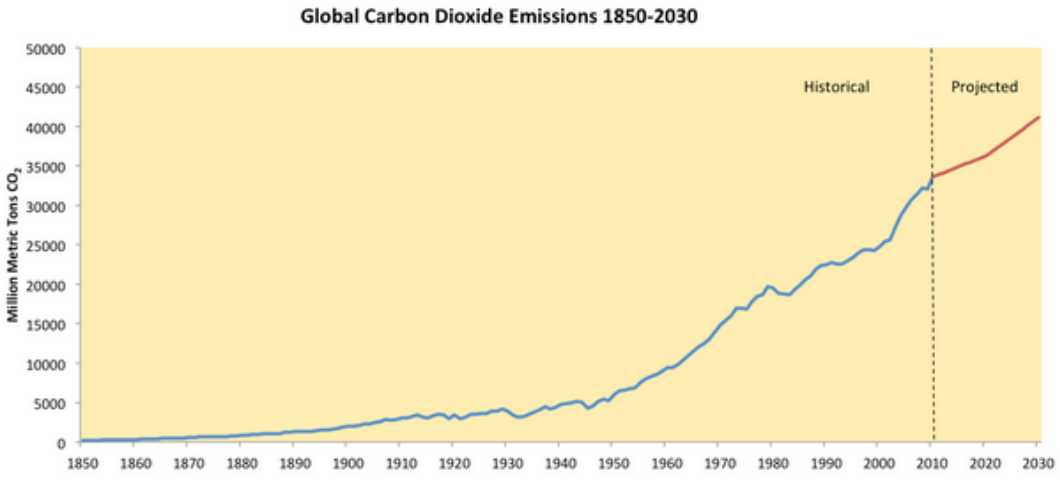

Figure 2: Global carbon dioxide emissions (6)

There are a lot of industrial processes that produce highly concentrated streams of CO_2 as a by-product. Fossil-fuel power production plants are the largest potential sources: 1000 MW of electrical power emit between 6 and 8 Mt/year of CO_2. (2).

In 2008, the countries with the most CO_2 emissions were China and the USA, including also the European Union (with 23, 19 y 13% of the total, respectively). These data include the emissions produced in fossil fuel combustion, cement manufacturing and gas flaring.

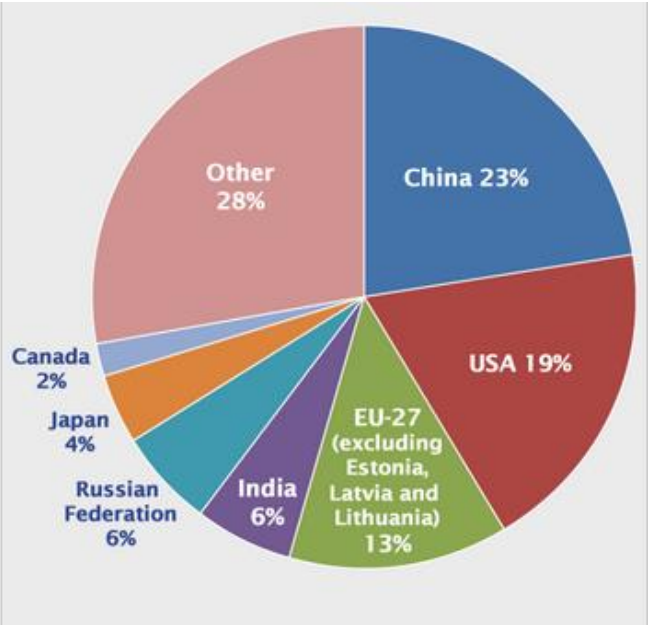

Figure 3: Emissions by country in 2008. (1)

2.2 Carbon capture and storage technologies

Carbon Capture and Storage (CCS) is one option to stop the global warming. It offers the opportunity to increase the demand of fossil fuel energy by reducing the greenhouse gases emissions, preventing its contribution to the climate change. Its principle application is in the power sector, refineries, synthetic fuel production, blast furnaces or cement kilns (7). Carbon capture and storage is formed by three main processes:

1) capture, purification and compression of CO_2 at the industrial process,
2) transportation to appropriate storage place, and
3) storage in a safe place.

The CO_2 capture is the most costly and most important stage (normally, 75% of the total costs). There are different ways to capture the carbon dioxide based on where this process is integrated in the power plant. They are classified in three groups:

1) Pre-combustion
2) Post-combustion
3) Oxyfuel-combustion

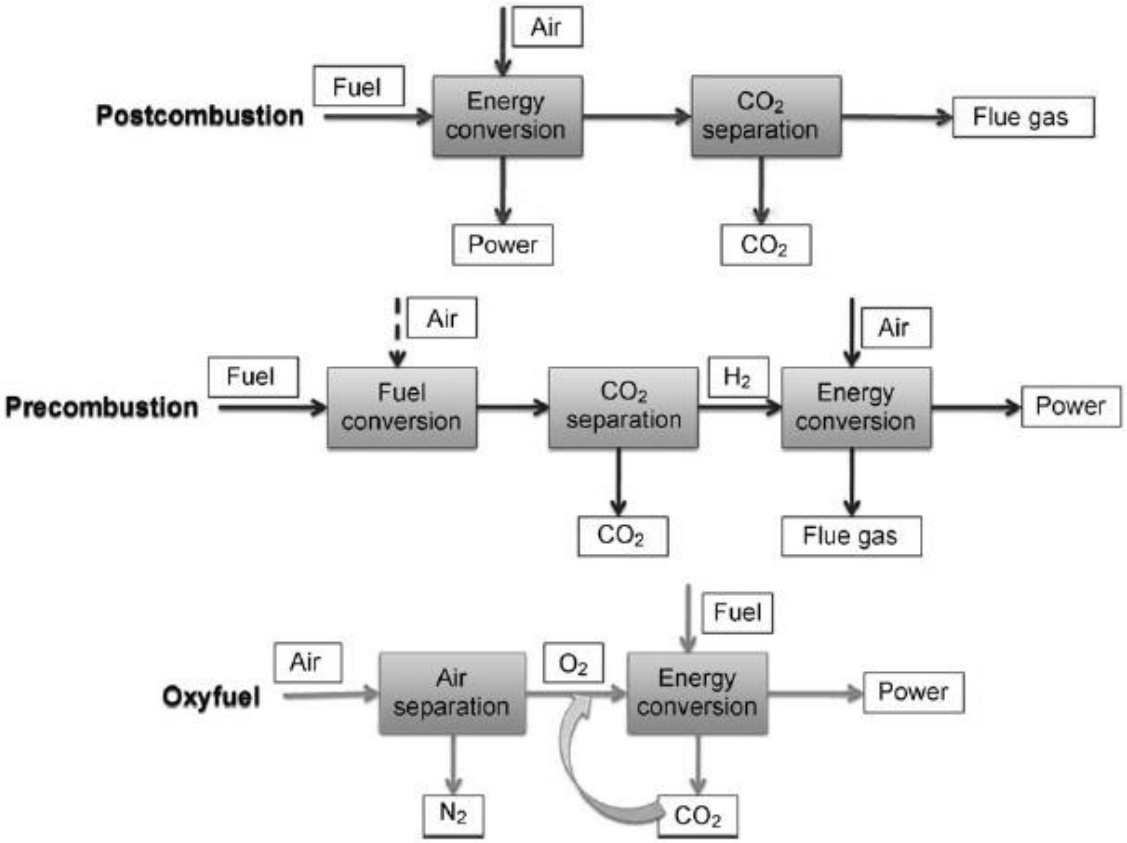

Figure 4: Different combustion processes (3).

The most important factors for selecting the capture system are the concentration of CO_2 in the gas stream, the pressure of the gas stream and the fuel type (solid or gas).

In **pre-combustion** processes, fuel reacts with oxygen or air giving mainly carbon monoxide and hydrogen; the process is called gasification. This reaction occurs before the fuel is burned. The mixture product (CO and H_2) is taken through a catalytic reactor, where CO reacts with steam forming CO_2 and more H_2. Then, the carbon dioxide is separated and the hydrogen can be used as fuel in a gas turbine combined-cycle plant. This process has two main advantages: the higher component concentrations and the elevated pressures reduce the energy capture penalty of the process to 10-16%, and the generation of a hydrogen-rich fuel, which can be used as a chemical feedstock.

The **oxyfuel-combustion** method is a modification of the post-combustion process. Oxygen and air are used as comburent gases. Nitrogen is completely excluded for the combustion process in a preliminary air separation step and then, the fuel is burned in an almost pure oxygen atmosphere. The product of combustion is a high concentrated stream of CO_2 (concentration of 80-98%) which is recirculated into the system. This method is considered a "zero emission cycle" in comparison with post-combustion method but on the other hand, it requires significant redesign of some equipment and it needs a large quantity of oxygen. So the retrofitting of existing plants is not economical, in terms of capital cost and energy consumption. For this reason, oxyfuel-combustion has only been demonstrated in small scale tests.

Finally, in **post-combustion** processes, the CO_2 is captured after fuel gas combustion. It usually applies to low concentrations of CO_2 (4-14%), such that it is necessary to handle large volume of gas, resulting in large equipment sizes and in an increase in the capital costs. The post-combustion processes can be applied in the majority of existing coal-fired plants (2).

By using CCS technology in a conventional power plant, CO_2 emissions could be reduced by 80-90% (3). The International Energy Agency (IEA) believes that using the CCS process in power generation could capture and store about 79 Gt of CO_2 between 2010 and 2050 (7).

The next figure shows a brief diagram of the different options with a diverse range of promising new materials for the CO_2 capture:

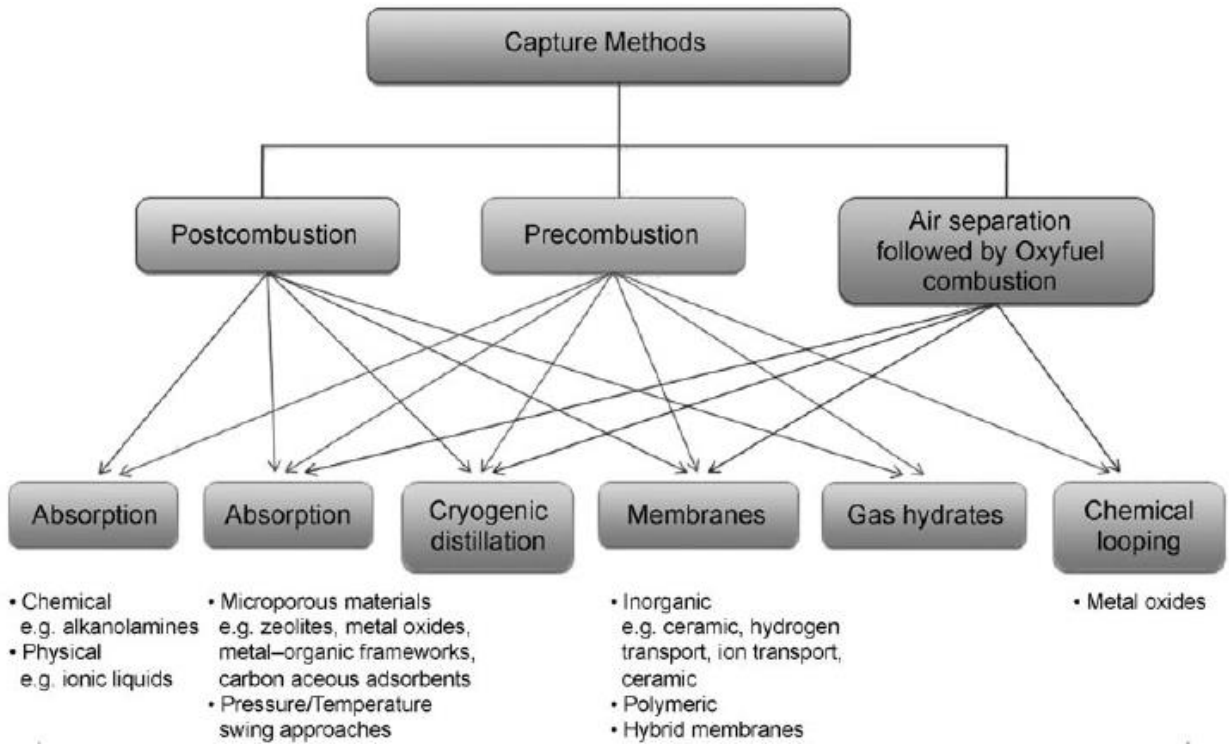

Figure 5: Materials for CO_2 capture in post-combustion, pre-combustion and oxyfuel processes (3).

For transportation, dedicated pipeline infrastructures are used, connecting the source plant with the storage site. The cost of this part is an order of magnitude less than for capture and the pipeline technology is well established and mature. So, the key issues in the transportation are about the sitting and the routes of pipelines, and the purity of CO_2 transported. Then, CO_2 can be stored in different locations, being the most developed the geological storage (in depleted oil and gas reservoirs or in deep saline formations). The costs of this stage are roughly equivalent to the costs of transportation, and some relatively constant costs across a big range of storage capacity exist (8).

Some methods investigated recently have used the adsorption of carbon dioxide. An efficient CO_2 capture must have the following characteristics (9):

- Large CO_2 adsorption capacity,
- Fast adsorption/desorption kinetics,
- Favorable adsorption and desorption temperature,
- Excellent cyclic stability.

The capture stage is the most costly and consumes a lot of energy, so the optimization of this technique is considered a very important issue. Sorbents with natural or synthetic materials have been tested for high temperature application. The characteristics desired in sorbents materials for the economic viability of CO_2 capture system are (10):

- High sorption capacity,
- Long-term durability,
- Fast sorption/desorption kinetic,
- Good mechanical strength properties.

Nowadays, calcium oxide based sorbents are being focused in different studies because of its low cost and wide availability in natural minerals.

2.3 Post-combustion: calcium looping cycle

The calcium looping cycle is based on the reversible gas-solid reaction between a calcium oxide sorbent (CaO) and carbon dioxide (CO_2) to form calcium carbonate ($CaCO_3$).

$$\Delta H_{r,298K} = -178\ kJ/mol$$

$$CaO_{(s)} + CO_{2\,(g)} \leftrightarrow CaCO_{3\,(s)} \quad \text{[eq. 1]}$$

CARBONATION (forward) / ***CALCINATION*** (reverse)

$$\Delta H_{r,298K} = +178\ kJ/mol$$

First, CaO is carbonated at high temperature (650-700 ºC) to $CaCO_3$ by an exothermic reaction, taking place a heat release which can be used in the CO_2 separation. Then, the calcium carbonate is regenerated to CaO by a calcination reaction (800-900 ºC), which is endothermic, releasing an almost pure stream of CO_2 again. Both reactions form a cyclic process, so after calcination reaction, the sorbent can be ready for the next cycle. The equilibrium vapour pressure of CO_2 over CaO can be represented as a function of temperature.

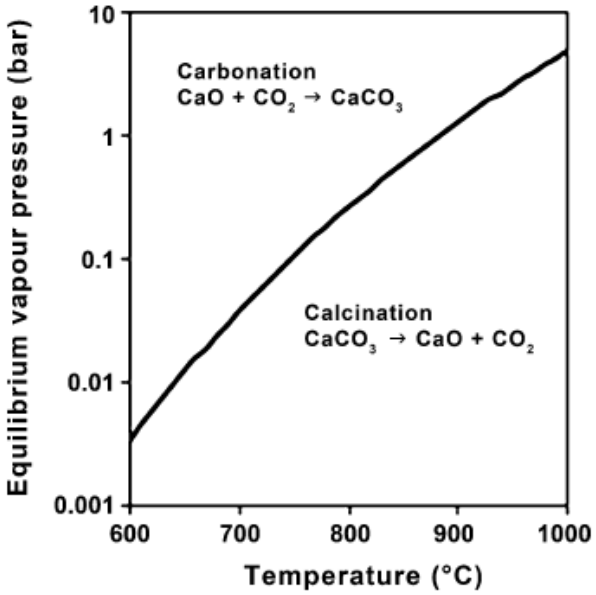

Figure 6: Equilibrium vapour pressure of CO_2 over CaO as a function of temperature (11).

In figure 6, it is shown that partial pressures of CO_2 higher than the equilibrium partial pressure at a given temperature will favour carbonation reaction and those lower than the equilibrium pressure will favour calcination reaction.

The important issue in CO_2 capture is to obtain a pure stream of carbon dioxide suitable for storage. The calcination temperature (800-900ºC) is due to the high CO_2 partial pressure necessary to form the pure stream, although the rate of calcination and the degradation of the sorbent are increased with high temperatures. The carbonation temperature (600-700ºC) is chosen as a compromise between the higher equilibrium capture (maximum) at lower temperatures and a decrease of reaction rate. The exothermic reaction involves two stages: the first one is an initial fast reaction rate controlled by the kinetics and the second one is a slower reaction rate due to the diffusion of carbon dioxide to the calcium carbonate product layer, which grows on the CaO surface, hindering the CO_2 absorption marking the start of the diffusion stage. (12)

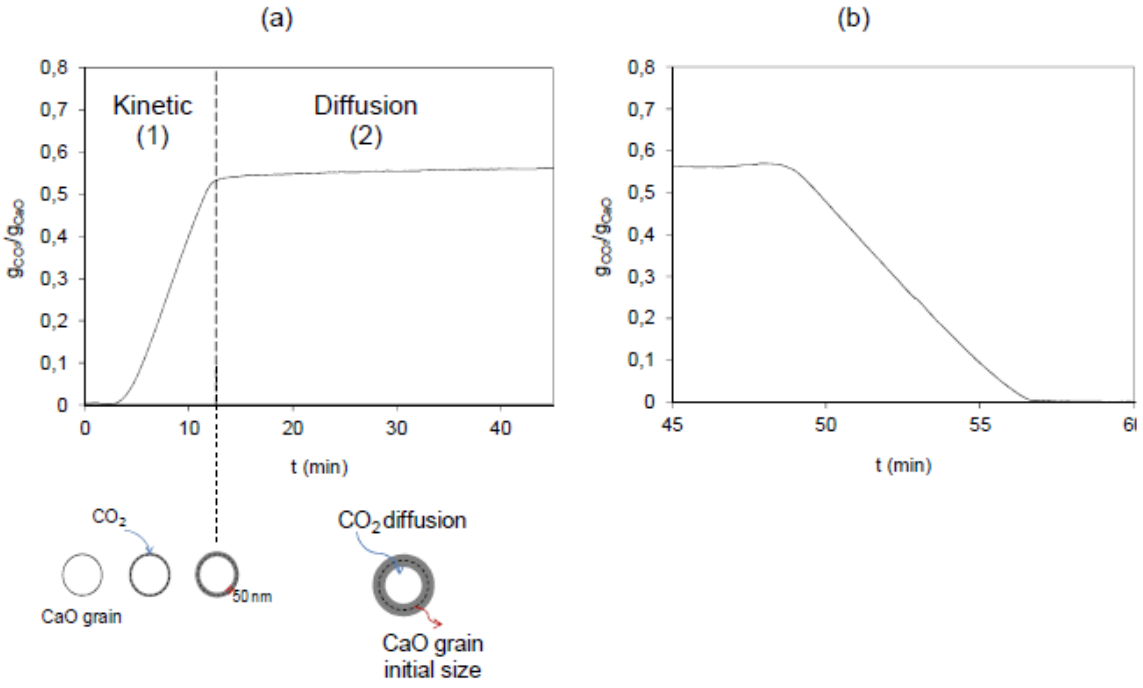

Figure 7: Evolution of the reactivity of a Ca-based sorbent in carbonation reaction (6.a) and in a calcination reaction (6.b) as a function of time (13)

In figure 7.a, the two stages of carbonation reaction explained above can be seen. First, the CO2 reacts on the CaO surface with a high rate of reaction (kinetics is controlling). Then, the diffusion stage starts controlling, with the formation of a CaCO3 layer on the surface of CaO (50 nm of thickness) restricting the access of CO2 molecules into the CaO particles.

2.3.1 Pilot plant trials for CaO-looping technologies.

Since not long time ago, there are several pilot plant projects for scaling-up Ca-looping technology and some of them include CO_2 capture system. The feasibility of the process has been confirmed through various tests at different scales. The first significant developed projects were carried out in Spain, Germany and Canada. In INCAR-CSIC (Spain), some experiments were performed in a continuously operated plant with 30kW, achieving CO_2 capture rates up to 85%. On the other hand, efficiencies greater than 90% were obtained in Stuttgart University (Germany). The tested plant had a 10kW capacity and the experiments were done under different combinations of operational parameters. Another 10kW plant was tested at CAEMET (Canada) operating in discontinuous mode, which showed the importance of humidity content as a very positive effect on carbonation step. In the same place, tests in a 75 kW process got 95% of CO_2 capture, decreasing to 71% after 25 cycles (11) (13) (14).

Recently, the most important initiative in the world to test the Ca-looping technology has been the project developed by European Union called *"Development of post-combustion CO_2 capture with CaO in a large testing facility: CaOling"*. It consists of scaling-up of the Ca-looping technology as a requisite for the pre-industrial demonstration plant. The calcium looping pilot plant has been built in the

50MW thermal central of group HUNOSA, in Oviedo (Spain). This pilot system has a capacity of 1,7MW and uses a side stream of flue gases of the commercial plant. The results show efficiencies between 50-95% achieved in CO_2 capture (13).

Between 2011 and 2012, a 1MW pilot plan at Technische Universität Darmstadt (Germany) was started up for the CO_2 capture investigation, implementing several improvements throughout the experiments, such as increasing the thermal power of the calciner (15).

2.3.2 Natural sorbents

One important natural sorbent is the limestone, which includes different carbonate minerals and fossils, composed of calcium and magnesium carbonates as well as some impurities like silica and alumina. In the next table, some of the compounds present in limestone are shown, being calcite the most abundant form:

Table 1: Normal composition of limestone (4)

Compounds	Formula
Calcite	$CaCO_3$ rhombohedral
Aragonite	$CaCO_3$ orthorhombic
Dolomite	$CaMg(CO_3)_2$
Magnesite	$MgCO_3$

Limestone with high quantity of calcite is the most used in studies about the CO_2 capture because of its initial highest uptake of CO_2 per unit mass and its low price. Dolomites have also been studied. They have a lower initial carbonation capacity but, after 20-30 cycles, its CO_2 uptake is better than in calcites. The excess of MgO in dolomites, which does not react during carbonation, keeps the porosity and, due to its higher melting point, sintering decrease during calcination stage, maintaining the porosity too (4). Both sorbents are available and cheap, although limestone with calcite is more abundant and it can be re-used as feedstock in the cement industry.

Capture capacity of natural sorbents decreases with increasing the number of carbonation-calcination cycles, being necessary a large amount of fresh limestone to keep an acceptable long term CO_2 capture efficiency. The main reasons are: sintering, attrition and sorbent deactivation (16). These factors are explained in detail in the next section.

a) Sintering

Sintering is directly related to a decrease of surface area. During heating, CaO particles suffer this phenomenon, taking place changes in pore shape, pore shrinkage and grain growth. This effect is constant during calcination and carbonation cycles, occurring mainly under high temperatures and durations of calcination. Higher partial pressure of CO_2 or some impurities are also factors that influence in sintering process. Several investigations have determined that sintering occurs in the

calcination step (4) and happens in a similar way in different limestones. Pore size evolution during carbonation-calcination cycles is often studied. *Shao et Al.* classified the pores in two groups: smaller pores (diameter < 220 nm) and larger pores (diameter > 220 nm), which were named as type I and type II, respectively., Pores of type I are formed after calcium carbonate calcination and pores of type II are produced due to the sintering of pores of type I. For this reason, surface area and pore volume in type I pores decrease while, on the other hand, pores of type II suffer an increase.

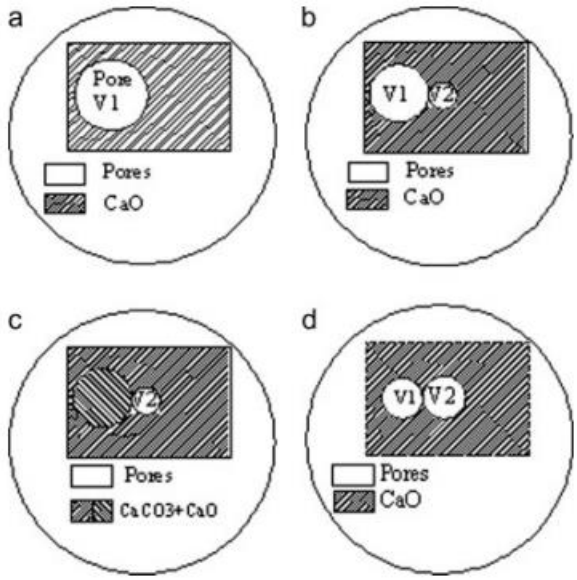

Figure 8: Scheme of sintering process (a) 1st calcination, without sintering; (b) bimodal pore distribution after sintering; (c) after calcination, smaller pores are filled; (d) after calcination and sintering, pores further develop (17).

Experimental results (figure 9) have shown that a bimodal distribution is developed after several cycles, where the smallest pores suffer shrinkage and the largest are prone to growing.

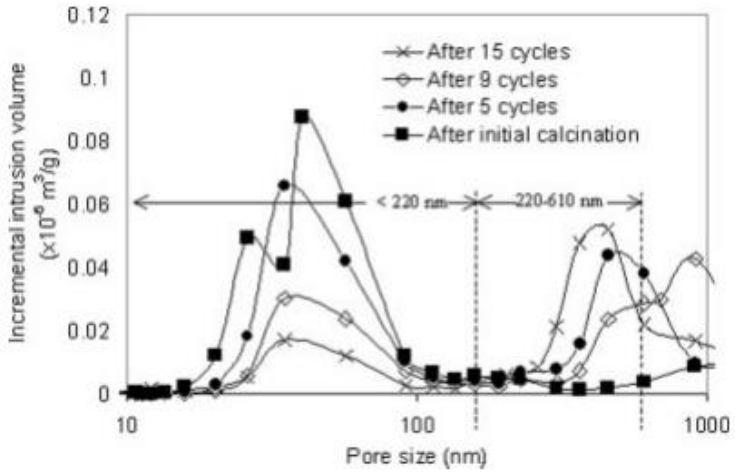

Figure 9: Pore size distribution after different carbonation-calcination cycles (17).

The mechanism of the grain growth is shown in the figure 10. It can be seen a representative scheme about the textural transformation of CaO sorbents over many cycles, in which the CaO is represented by light grey and the $CaCO_3$ by dark grey.

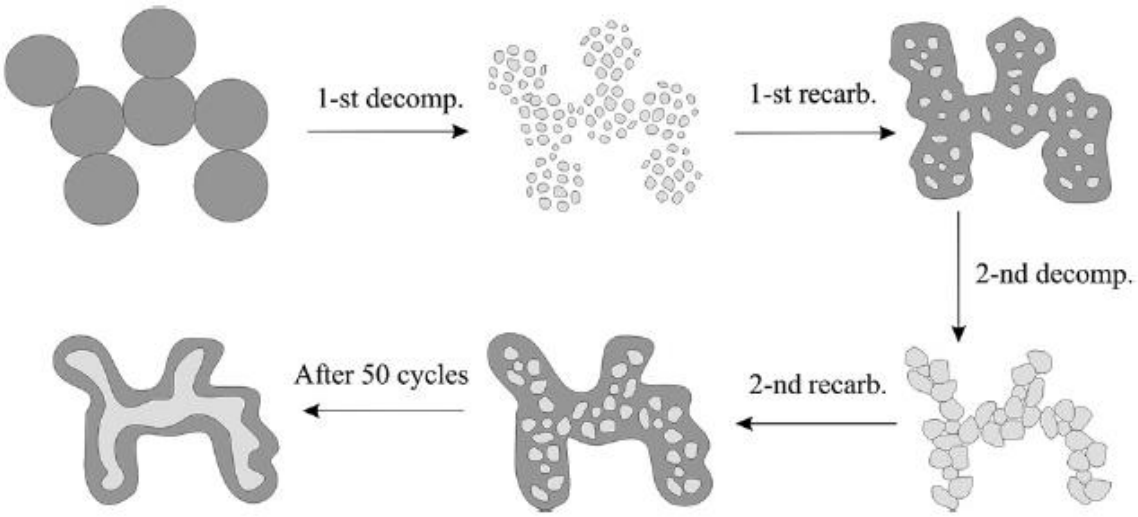

Figure 10: Grain growth in CaO sorbents after several carbonation-calcination cycles (4).

After first calcination, CaO is formed in an extremely dispersed way, being highly reactive. The next carbonation is not carried out completely due to pore blocking after carbonation and sintering process. Then, several pores do not open again in the next calcination, and this process occurs continuously until the formation of a rigid block after many cycles. A decrease in the surface area and in the reactivity of the sorbent is observed.

b) Sorbent deactivation

Sorbent efficiency can be measured by the carrying capacity, defined in the next equation. It is expressed in terms of grams of CO_2 adsorbed in each cycle per grams of initial calcined sorbent.

$$carrying\ capacity = \frac{g\ of\ CO_2}{g\ of\ calcined\ \ sorbent} \qquad \text{[eq. 2]}$$

Taking into account the molecular weights of CaO and CO_2, it is known that 1g of CaO would capture 0,786 grams of CO_2. This ratio is only in a stoichiometric way, since in natural CaO sorbents occurs the pore-filling and pore blockage due to the $CaCO_3$ formation, limiting the CaO conversion and the carrying capacity (18). Therefore, this value is taken as 100% conversion of calcium oxide, corresponding to the maximal theoretical carrying capacity of a sorbent.

Many experimental studies have determined that natural sorbents uptake decays rapidly, after they are subjected to repeated carbonation-calcination cycles.

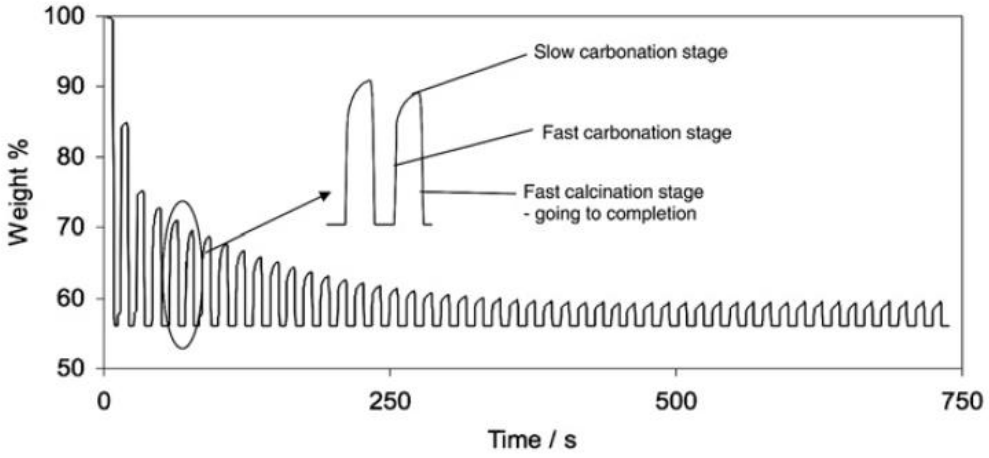

Figure 11: Cycling experiment performed in a thermogravimetric analyser (4)

Figure 11 represents these cycles in a limestone carried out in a thermogravimetric analyser under 15% in volume of CO_2. The reactions took place between 900ºC and 650ºC. After the first calcination (decreasing the sorbent mass from 100% to ~56%), a quickly carbonation occurs, followed by a slow carbonation period, and finally the calcination step is taking place again. It can be seen that while the mass after calcination step is approximately constant, the mass after each carbonation period decays rapidly along the cycles. For that reason, the reactivity of natural sorbents is reduced to an asymptotic value of ~8% of the initial.

The main factors influencing the sorbent degradation reactivity are (11): CaO porous sintering occurred during calcination step; competing of sulphation/sulphidation reactions; loss of bed material through attrition causing the elutriation of fines; and ash fouling. As it has been explained in the previous section, CaO is prone to sintering in Ca-looping process, limiting its reactivity.

Calcium oxide has a very strong affinity with SO_2, being used as a sorbent for sulphur oxide in industrial processes. It is an excellent desulfurization agent, producing $CaSO_4$ in an irreversible way at temperatures and atmospheres typically used in post-combustion processes. Two reactions can take place:

$$CaO(s) + SO_2(g) + {}^1/_2\, O_2 \rightarrow CaSO_4(s) \qquad \Delta H^\circ = -520\ kJ/mol \qquad \text{[eq. 3]}$$

$$CaCO_3(s) + SO_2(g) + {}^1/_2\, O_2 \rightarrow CaSO_4(s) + CO_2(g) \qquad \Delta H^\circ = -324\ kJ/mol \qquad \text{[eq. 4]}$$

There are several investigation works about this phenomenon and its influence in the decay of CO_2 carrying capacity of some sorbents.

In a typical system, the fuel combustion in the calciner causes two effects: on the one hand, fine ash and chars are introduced into the system, depositing on the particles surface which produces undesirable side reactions and the formation of a low temperature melt; and on the other hand, there are higher local temperatures because of the combustion (11) (19).

In recent years, several options have been investigated in order to decrease the handicap of loss carrying capacity in calcium looping. The main options are (10) (19):

- ***Reactivation of CaO by steam hydration:*** achieving an increase in the pore volume and in the cycle performance. The formation of $Ca(OH)_2$ and its following calcination produce a high reactivation of the sorbent for carbon dioxide capture.
- ***Pre-activation and self-reactivation effects:*** in this method the purpose is getting a more stable pore texture with a controlled pre-calcination of the sorbent. It is a promising technique but recent investigations have not found relevant benefits in precalcination.
- ***Sorbent doping of natural materials:*** there are not positive conclusions about this option, and in addition, many of the dopants studied could not be compatible with safe coal power plant operation.
- ***CaO recarbonation:*** it consists in the incorporation of another reactor, forming a carbonation-recarbonation-calcination cycle. The idea is obtaining a residual CO_2 carrying capacity higher than in a conventional carbonation-calcination system.
- ***Synthetic sorbents:*** nowadays, a huge variety of precursors, supports and binders for calcium oxide have been investigated. In the next section, this method is explained in depth.
- ***Activated carbon as structuring in sol-gel synthesis:*** the use of activated carbon in synthesis of CaO sorbents increases the porosity in the sorbents, mitigating the deactivation effect over cycles of carbonation and calcination. Results about this technique can be seen in the previous thesis of Joana Fernandes Hipólito (20)

2.3.3 Synthetic sorbents

Synthetic sorbents have also been synthesized and tested for CO_2 capture, in order to improve the problems with the deactivation of natural sorbents. They are called CaO-based sorbents and can incorporate different additives which increase the capture capacity and the mechanical stability (16).

The most used methods for improving the carrying capacity and stability of CaO-sorbents are the incorporation of inert materials and the modification of the pore structure (10). The inert material more commonly incorporated into the sorbent is MgO, however the use of a large amount of inert component produces an increase of tank capacity and operating costs, thus being unfavourable. Other

inert materials have been studied, such as alkali metals or $CaTiO_3$. Pore structure modification is another strategy for improving the stability of sorbents. The most typical way is the precipitated calcium carbonate (PCC). Recently, mesoporous silica solids have been used as supports because of their numerous advantages, which will be analyzed in the next section.

Sorbents can be prepared in different ways, studying the behavior of various supports and additives.

a) Synthesis methods of CaO-based sorbents

Synthetic sorbents can be obtained mainly by two methods: one is the precipitated calcium carbonate, and the other is the sol-gel method, in which sorbents can be supported or not.

a.1) Precipitated Calcium Carbonate (PCC)

Florin, Blamey and Fennell (16) carried out a novel precipitation method which consists in the production of CaO-based sorbent incorporating an inert mixed calcium-aluminum oxide binder. These synthetic sorbents present highly reactive and highly resistance to sintering compared with those derived from natural limestone. The process is based in the reaction of dissolved CO_2 gas and calcium ions (Ca^{2+}) derived from natural limestone, which is performed in a slurry bubble column. The mixed precipitation occurs due to the higher solubility of $Ca(OH)_2$ than $CaCO_3$ (0.12 and 0.0013g/100mL, respectively). Some carbon dioxide gas is dissolved when it is bubbled through the slurry column, forming carbonate ions (CO_3^{2-}) which react with Ca^{2+} ions producing the $CaCO_3$ precipitation. Initially, when the OH^- concentration is very high, the Al^{3+} ions react with H^+ ions and precipitates in $Al(OH)_3$ form. The next figure shows a representative scheme of the slurry bubble column used in the synthesis. After the synthesis process, the precipitated mixture is accumulated and transferred directly into an oven for drying overnight at 120ºC.

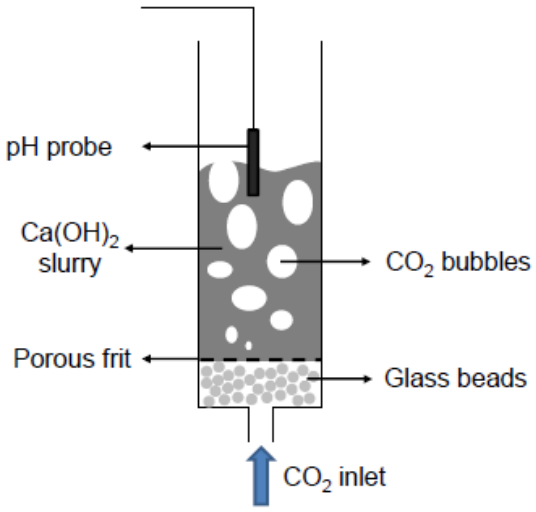

Figure 12: Scheme of the slurry bubble column

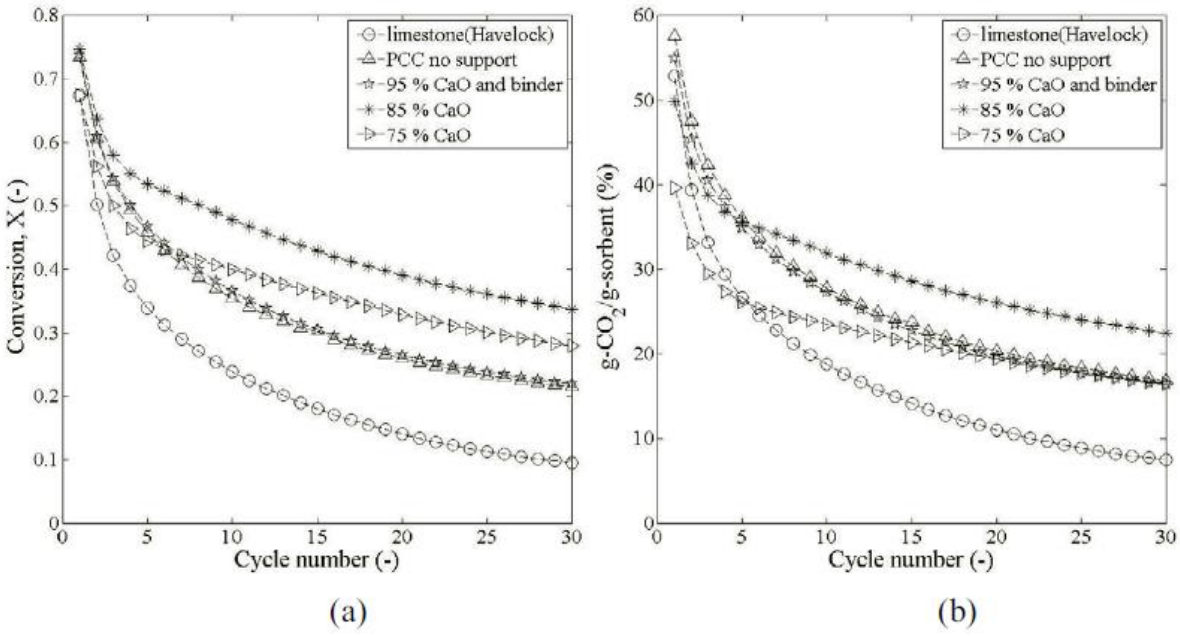

Figure 13: Carrying capacity of synthetic sorbents after 30 cycles, expressed in (a) conversion; and (b) g CO_2/g sorbent (21).

Figure 12 shows the carrying capacity of different synthetic sorbents compared with natural limestone and CaO derived from precipitated $CaCO_3$ without binder. The synthetic sorbents are loaded with binder from 0-25 wt%. It can be seen that the carrying capacity of the synthetic sorbents is superior to the natural limestone, but it is important to emphasize that the capacity of the sorbent with 85% of CaO and binder is about 3 times more after 30 cycles. During the first 5 cycles, all modified sorbents experiment a fast rate of decay due to the irreversible formation of the mixed precipitation. After, the rate of decay is more gradual, indicating the complete conversion of Al_2O_3 (16) (21).

a.2) Sol-gel method

This method allows the synthesis of synthetic sorbents with high surface area and reactivity; however it is a slow preparation process, with higher costs than natural sorbents. For that reason, the implementation in industry is more difficult.

Xu et al. (22) investigated the synthesis of different CaO-sorbents by sol-gel method with several calcium precursors, such as calcium acetate, calcium citrate, calcium lactate, calcium gluconate and acetic acid. Inert $Ca_9Al_6O_{18}$ was used as support matrix. In the next figure, the main textural properties of the sorbents prepared are shown:

Table 2: Textural properties of CaO-based sorbents (70, 80, 90 wt% CaO)
CA: calcium acetate; CC: calcium citrate; CL: calcium lactate; CG: calcium gluconate (22)

Sorbent	BET surface area (m^2/g)	Volume (cm^3/g)	Pore diameter (nm)
CA-80	9.89	0.029	18.4
CC-80	9.64	0.030	13.4
CL-80	11.15	0.042	19.7
CG-80	8.37	0.028	20.9
CL-70	10.06	0.039	24.0
CL-90	10.86	0.036	15.3
CaO	7.43	0.039	30.8

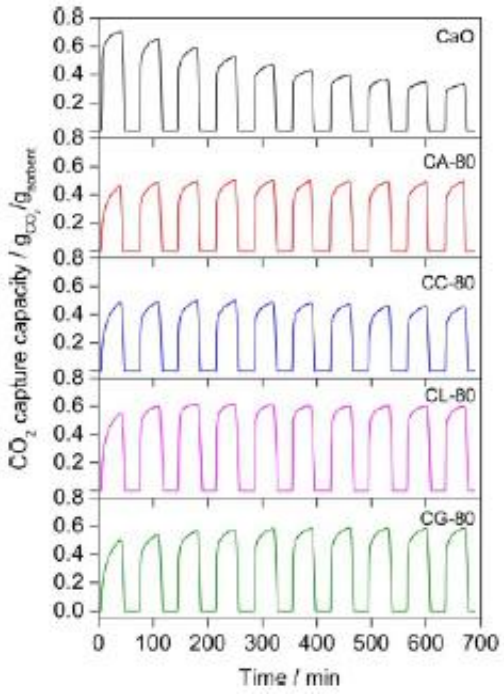

Figure 14: Capture capacity of the different sorbents (22)

Some of these samples were tested for the CO_2 capture, in order to study the evolution of their carrying capacity as a function of time. They were subjected to 10 carbonation-calcination cycles at 650 and 800ºC, respectively. In figure 14, it can be seen that the carrying capacity decreases in the pure CaO sample through the cycles, while in synthetic sorbents, the capacity remains constant. The best results were achieved in samples with 80 wt% CaO in calcium lactate and calcium gluconate.

Santos et al. (12) used a modified Pechini procedure (sol-gel method) to prepare several synthetic sorbents with highly surface area which are more resistant to sintering effect through carbonation-calcination cycles. With the purpose of studing the sorbent deactivation, they carried out an experiment with 70 cycles.

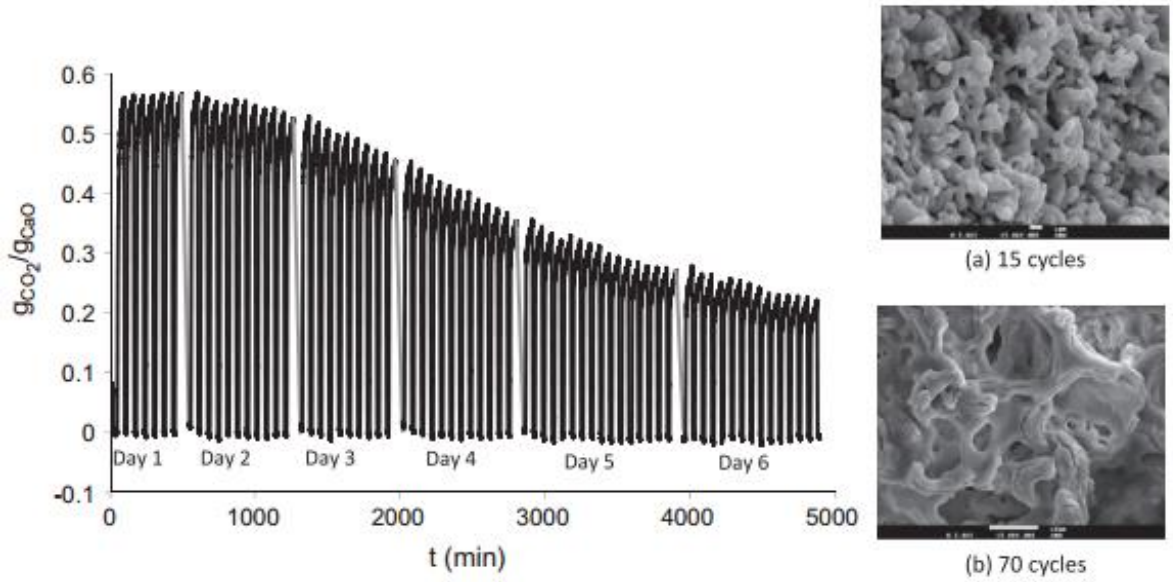

Figure 15: Carbonation-calcination experiment to study the carrying capacity of sol-gel CaO sorbents. SEM images: (a) CaO after 15 cycles; (b) CaO after 70 cycles (12)

The results show that in the first 18 cycles only a 5% of loss capacity took place and, although the carrying capacity suffered a pronounced decrease during the experiment, the final value after 70 cycles (~0.24 gCO_2/gSorbent) was three times more the capacity observed in natural limestone (0.08 gCO_2/gSorbent). In figure 15, it is also shown two SEM images of carbonated samples, in order to study the synthetic sorbents behavior. After 70 cycles, the structure is less ramified than for 15 cycles. There are some cavities in the second image, which maybe appeared because of CO_2 during calcination reaction (12).

2.3.4 Mesoporous supports

Three types of porous materials exist, depending of the size of the pore: micropores (< 2 nm), mesoporous (2-50 nm) and macroporous (> 50 nm). Mesoporous materials are defined by IUPAC as materials with pore of free diameters in the range of 2-50 nm. They are preferred as supports due to several reasons:

1) Highly ordered mesostructure,
2) High surface area and pore volume, allowing the diffusion and adsorption of different molecules for wide applications.

The most common applications of mesoporous materials are: catalysts and catalytic supports, drug control delivery, biosensors, biofuel, adsorption and membrane separation.

Silica is widely used as building block of these materials because it is not expensive, thermally stable, chemically inert, harmless and it is abundant in the Earth crust.

The two most known types of mesoporous materials are MCM-41 and SBA-15. The first one was discovered in 1990 and it was the most popular in researches concerning mesoporous materials. Since then, different types of these materials were developed and are known as M41S family. In 1998, SBA-15 (Santa Barbara Amorphous-15) appeared in a study which produced a material consisting in an hexagonal array of pores, being a huge development in mesoporous field (23), especially because of its large pores size when compared with conventional MCM-41 materials.

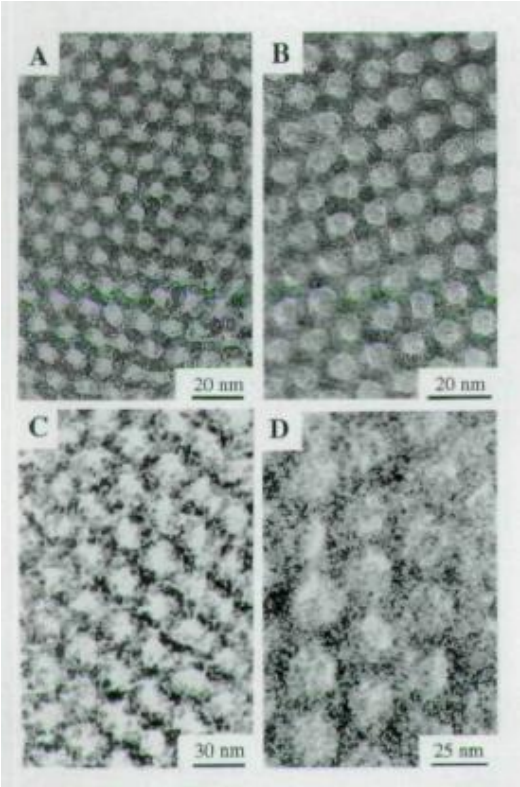

Figure 16: TEM images of calcined hexagonal SBA-15 with different pore size (60, 89, 200 and 260 Å) (24)

Some of the advantages that make SBA-15 preferable over other types of supports are (10) (23):

1) large pore size (4.6-30 nm)
2) thermal, mechanical and chemical resistance properties
3) high surface area
4) good performance
5) easy synthesis
6) thick pore wall

The most common synthesis of SBA-15 is carried out using triblock copolymers, typically non-ionic compounds, as structure directing agent or template, and tetraethyl orthosilicate (TEOS) as silica precursor. The template dissolved into the aqueous solution leads to the formation of an ordered mesoestructured composite during the condensation with the silica source. The porosity in the matrix is generated by subsequent removal of the surfactant by calcination or extraction (23) (25). The different synthesis steps will be explained in the next section.

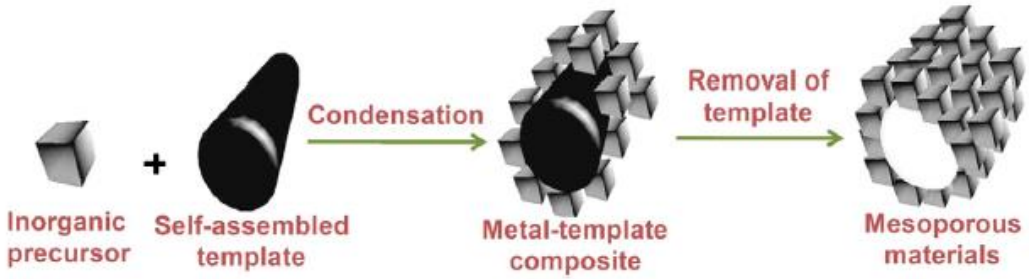

Figure 17: Scheme of the formation of mesoporous solids. (25)

Surfactants have hydrophobic and hydrophilic components in the molecule. In non-ionic surfactants, the hydrophilic components are non-dissociable.

Pore formation, along with its size, shape and dimension, depends on the surfactant supramolecular self-aggregation, being some factors very important: nature of template molecule, temperature, the concentration of the surfactant or the role of the sorbents. The nature and the concentration of surfactants have large impact on the size and shape of the self-assembled superstructure.

There are two different mechanisms about the formation of mesoporous materials. The first mechanism is known as "**cooperative self-assembly**" and it consists in a simultaneous aggregation of the template with the inorganic material, that has been already added. A liquid-crystal phase with a particular arrangement (hexagonal, cubic or laminar) can be developed, containing the organic micelle and the inorganic precursor. The second mechanism is called "**true liquid crystal template**". A lyotropic liquid-crystalline phase is formed before the addition of the inorganic species. The reason is the high concentration of the surfactant in the aqueous solution. The figure 18 shows both mechanisms explained above:

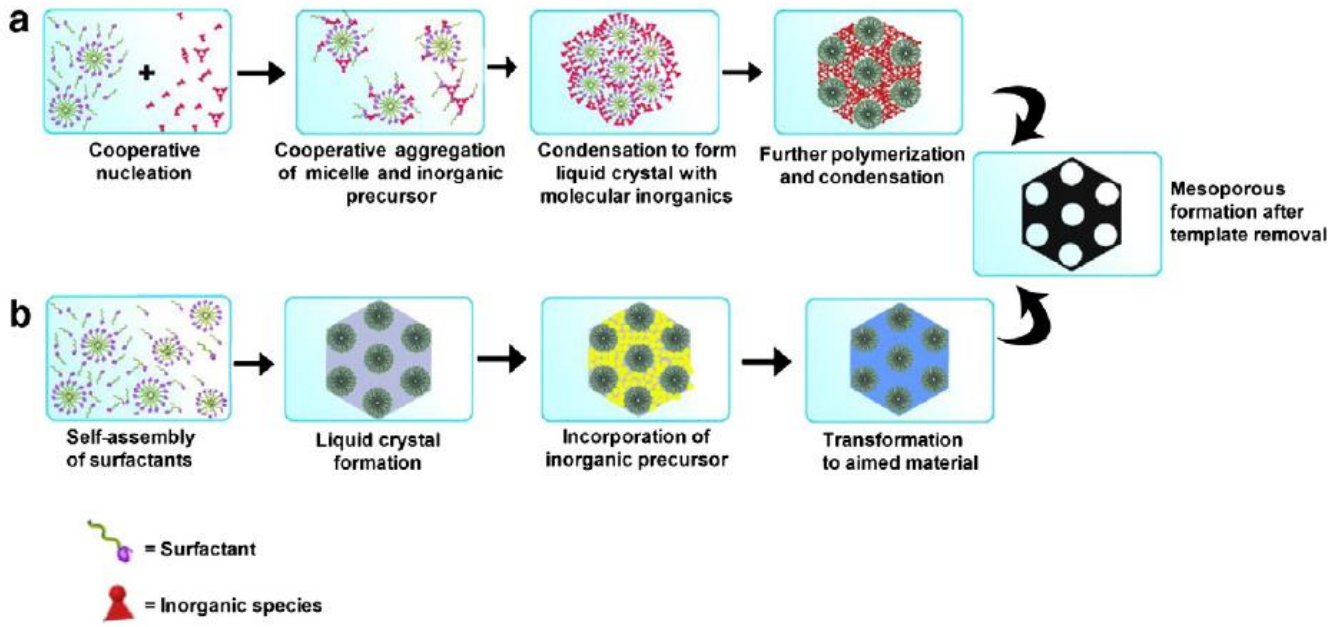

Figure 18: Mechanisms of mesoporous formation: (a) cooperative self-assembly, (b) true liquid crystal template. (25)

For the development of the mesoporous material porosity, it is necessary to remove completely the template of the compound. This step is carried out after the formation and condensation of the inorganic-organic material, creating a composite called as-synthesized material. The most particular method to eliminate the template is by calcination.

In general, a typical ordered mesoporous silica synthesis consist in two steps: the first, self-assembly of silica and template species, takes places under vigorous stirring at a low temperature; and the second step (mesoporous expansion and siliceous consolidation pore walls), is the hydrothermal treatment which occurs under static conditions at a higher temperature.

Since 1992, several methods have been carried out for the synthesis of SBA-15, being the most popular the microwave-assisted method. The use of microwave is growing up recently due to different advantages (26) (27):

- Rapid and homogeneous heating of the entire sample throughout the reaction vessel,
- Possibility of selective heating according to the desired conditions,
- Improve the reaction rates,
- Easy formation of uniform and homogeneous nucleation centers,
- Efficient way to control particle size distribution and morphology,
- Energy efficient and environmentally friendly.

The most important difference between conventional and microwave processes is that the latter reduces the total time from days to hours, without getting worse the final quality of the product, and also permits to program time and temperature of consecutive steps easily. Several investigations have been performed to compare both methods.

Jaroniec et al. (27) carried out the comparison of SBA-15 synthesized at 180ºC under microwave and conventional conditions. They also analyzed the duration of the hydrothermal treatment (1 and 3 hours). The results showed that the conventional SBA-15 has higher surface areas (~700-900 m^2/g) than with microwave method (~500 m^2/g), because the complementary porosity (mainly micropores) is reduced during microwave treatment. In figure 15, it can be seen that in conventional method, the surface area and the pore size distribution increase when the hydrothermal duration increases, while with microwave synthesis, theses parameters remain more or less similar.

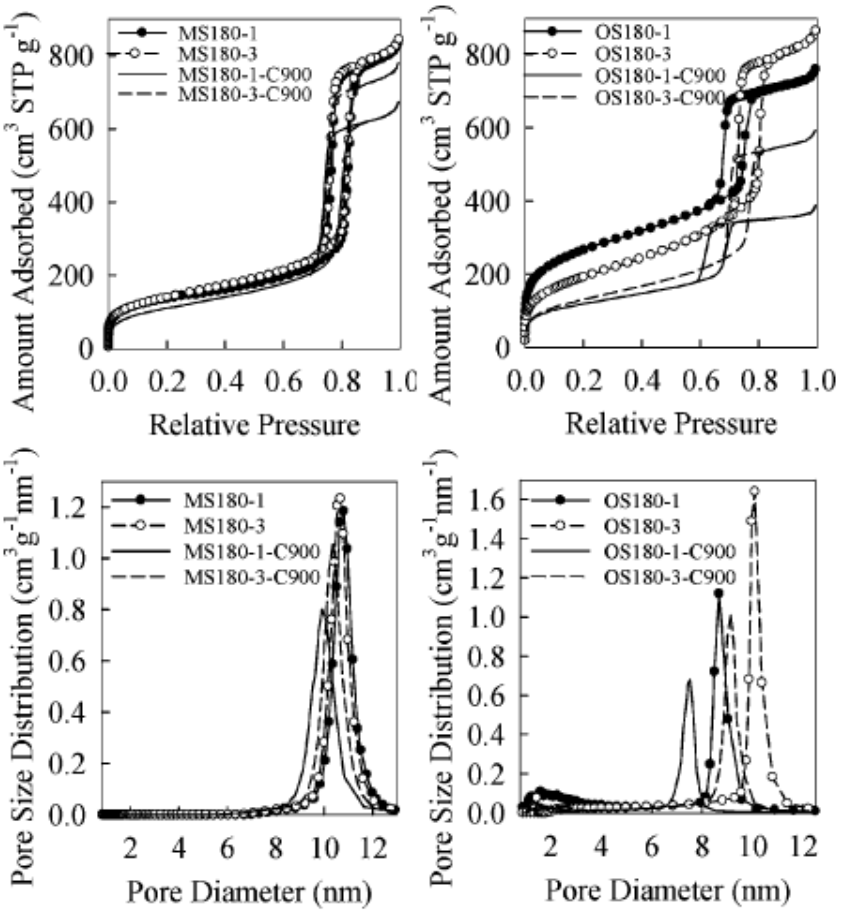

Figure 19: N_2 adsorption-desorption isotherms and pore size distribution for SBA-15 samples synthetized by microwave (MS180) and conventional (OS180), calcined at 540 and 900ºC (27).

Others studies, such as from *Lebeau et al.* (28), investigated the influence of different parameters in the synthesis of SBA-15, concluding that 2 hours is an optimum crystallization time using a microwave system during the hydrothermal treatment.

3 MATERIALS AND METHODS

This chapter presents all the synthesized samples (sorbents and supports), along with the methods of preparation. Then, the sorbents were characterized with different techniques, namely powder X-Ray Diffraction (PXRD), nitrogen sorption measurements, and thermogravimetric analysis (TG-DSC), which are also described in this section.

3.1 Sorbents and supports

In the next tables, the different sorbents and supports synthesized and their methods of preparation are shown:

Table 3: Synthesized supports

SUPPORT	SYNTHESIS METHOD	STRUCTURANT
SBA-15	Microwave	Pluronic P123
SBA-15	Classic Method	Pluronic P123

Table 4: CaO-based sorbents synthesized

SAMPLE	SYNTHESIS METHOD	STRUCTURANT
Ca/SBA-15	Dry Impregnation	Pluronic P123
Calcium Oxide	Sol-Gel Method	-
Calcium Oxide	Sol-Gel Method	Activated Carbon
Calcium Oxide	Sol-Gel Method	Carbon BP2000

3.2 Supports synthesis

Two different ways have been used for the support preparation: classical method and microwave-assisted synthesis.

3.2.1 Classical method

For the mesoporous silica SBA-15 synthesized using the classical method, the first method described by *Zhao et al* (29) was followed. The triblock copolymer P123 used as a structure-directing agent is dissolved in distilled water, where HCl solution (37%) was previously added (acidic media). The mixture was stirred overnight. Next, the solution is heated during 4 hours at 40ºC and then, the required amount of TEOS (silica-source) is added dropwise to the solution with continuously stirring and at 40ºC during 2 additional hours, allowing the hydrolysis of TEOS and formation of an homogeneous reactive gel. The gel product is transferred into a propylene bottle and is aged at 100ºC for another 48h without stirring. After that, the final mixture is filtered, washed with distilled water until

a neutral pH is been got, and dried at 100ºC overnight in an oven. SBA-15 is obtained after calcination in a required temperature for 10 hours with a heating rate of 2ºC/min.

3.2.2 Microwave-assisted synthesis

This process is the same as the classical method explained above, although with one difference: hydrolysis of TEOS and crystallization of SBA-15 are carried out under microwave-hydrothermal conditions.

The microwave equipment used is a Microwave-Accelerated Reaction System (MARS-5), which is commonly use to digest, dissolve and hydrolyze a wide variety of materials in the laboratory scale. The system uses microwave energy to heat samples quickly at elevated pressures. The system is formed mainly by (30) (31):

- A power system that allows users to select the desired power (300, 600 or 1200 Watts). In this work, all samples have been prepared using 600 Watts.
- A programmable microcomputer that controls and monitors the power, temperature and pressure inside the vessels, using temperature and pressure sensors.
- A turntable in where autoclaves are arranged. It rotates so that a homogeneous heating throughout all vessels can be obtained.
- Twelve autoclaves which are composed primarily by a Teflon reactor vessel, a Kevlar explosion proof sleeve, a vessel tap with a pressure rupture disc between the port in the vessel tip and the grey cap, and the structure where vessels are held in the turntable. All autoclaves are similar except one, in which temperature and pressure are measured with a fiber optic sensor and a pressure transducer, respectively.

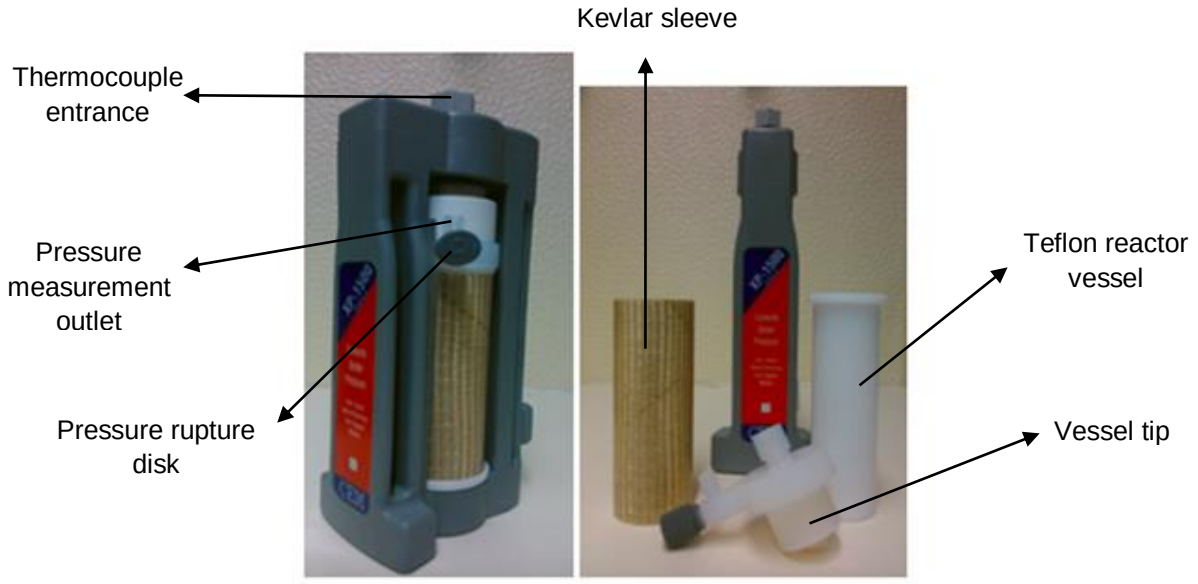

Figure 20: Scheme of microwave autoclave in microwave-assisted synthesis.

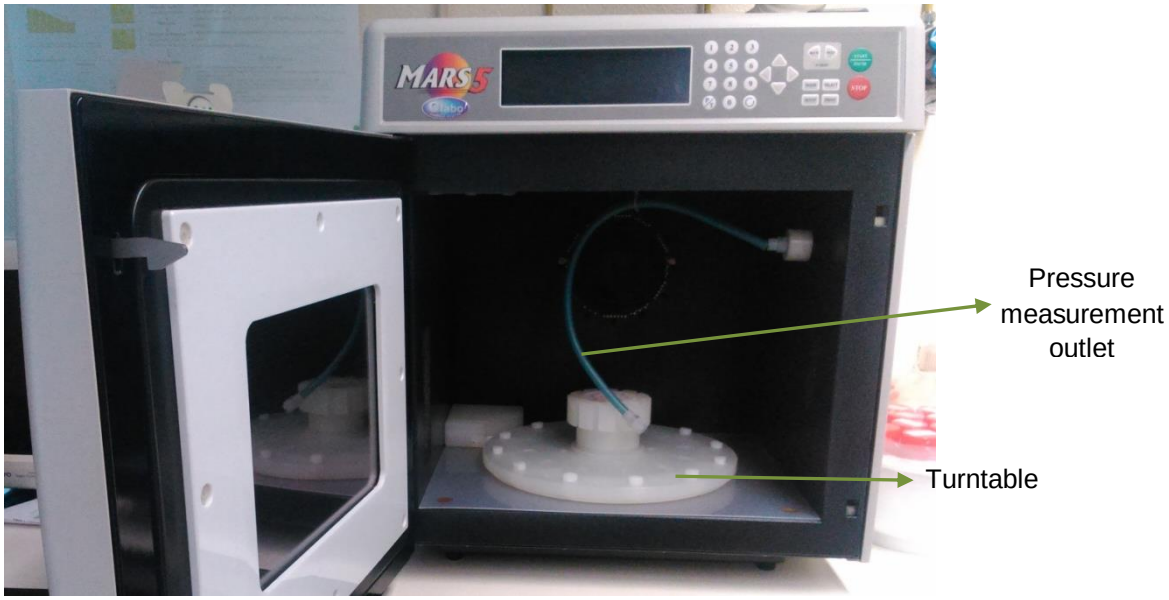

Figure 21: Microwave-Accelerated Reaction System (MARS-5) from CEM company.

After TEOS addition into the solution and subsequent stirring, the resulting homogeneous mixture has to be divided into equal parts and transferred into the autoclaves that are placed in the microwave oven at desired temperature and time. Autoclaves have to be introduced inside the microwave, in the right position, so as to be balanced. The final products are filtered-off, washed with distilled water until a neutral pH is reached and dried at 100ºC overnight in an oven. SBA-15 is obtained after calcination at 550ºC for 10 hours with a heating rate of 2ºC/min.

3.3 Sorbent synthesis

Synthetic sorbents have been prepared following two different methods: sol-gel method and wet impregnation of SBA-15 supports. The first one was applied for the preparation of calcium oxide sorbents and the second for the preparation of supported CaO sorbents. Both are explained in this section.

3.3.1 Sol-Gel method

These samples were synthesized in order to follow the research work of Joana Fernandes Hipólito *"Influência das condições operatórias na síntese de adsorventes à base de CaO com carvão ativado na Captura de CO_2."* (20).

The calcium source used in this method was calcium nitrate tetrahydrate (Ca(NO3)2·4H2O), which was mixed with citric acid monohydrate (C6H8O7·H2O) as complexing agent and distilled water as solvent. In two samples, different mesoporous-structuring agents were added: activated coal and carbon BP2000. Activated carbon (Norit GAC 1240 plus) is a granular activated carbon of high purity produced by steam activation of select grades of coal (32). Carbon BP2000 (black pearl) consists in

uniform, spherical carbon particles of about 50 nm in size .Sol-gel method includes these main three steps:

a) Sol-Gel formation

In this step, the solution is prepared with the predetermined amount of reagents. The mixture is continuously stirred and kept at 60 ºC. After 3-4 hours, particles start precipitating and finally the gel is formed. The gel formed is white while in the synthesis of sorbents with activated carbon as structurant the gel is black.

b) Drying step

The wet gel formed is dried into an oven, overnight at 130 ºC. After the drying step, it was observed that the sample without structurant presents a yellow color and the volume occupied is much less than with the other samples (with activated carbon as structuring agent), which present a greyish color.

c) Calcination

The sorbents were calcined in a muffle furnace at 750 ºC for 5 hours, with a heating rate of 2ºC/min. All samples presented a white color after calcination.

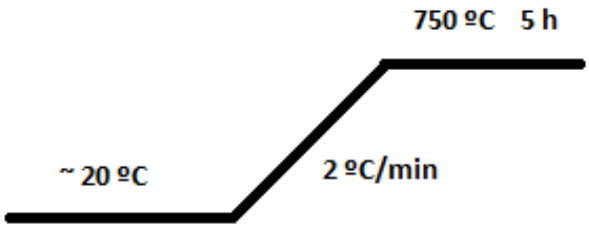

Figure 22: Scheme of calcination process

3.3.2 Incipient wetness impregnation

The CaO sorbents supported in SBA-15 were prepared by incipient wetness impregnation. This technique consists in mixing the support with a solution of the calcium source, using the exact amount of solution corresponding to the pore volume of the sample. First, a solution of the calculated amount of Ca precursor is prepared with distilled water and is added to the support, which is placed into a beaker previously. It is necessary to add the Ca precursor solution drop by drop, until the solid mixture turns into a malleable paste. Then, the paste formed is dried in an oven at 130 ºC overnight. Finally, the resulting sample is calcined in a muffle furnace at 550 ºC for 10 hours, with a heating rate of 2 ºC/min.

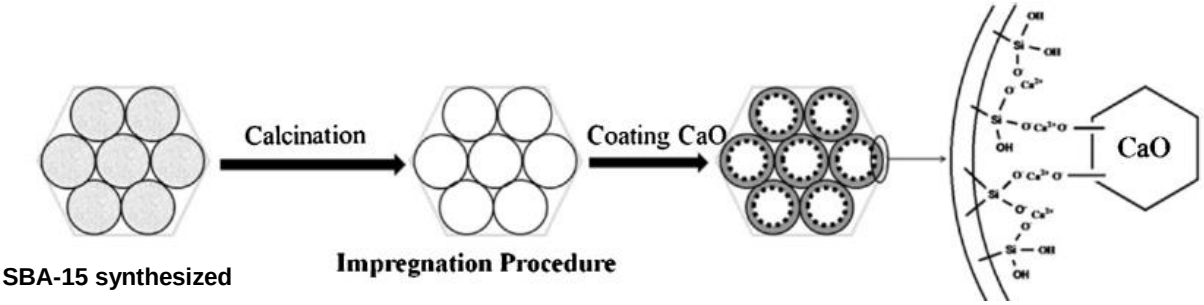

Figure 23: Schematic diagram of the impregnation process (33)

3.4 Characterization techniques

After the preparation step, all sorbents were characterized by several techniques: thermogravimetric analysis (TGA-DSC), powder X-Ray diffraction (PXRD), and nitrogen sorption measurements. In this section, the different techniques are presented.

3.4.1 Thermogravimetric Analysis (TGA) and Differential Scanning Calorimetry (DSC)

Thermogravimetric analysis technique allows the monitoring of the mass variation in the sample with temperature along the time under a controlled atmosphere (nitrogen or air). Differential scanning calorimetry is used to assess the nature (endo or exothermic) of the different processes associated with mass changes. The procedure consists in the introduction of the sample into a platinum crucible, which is suspended into a rod coupled to a microbalance, together with an empty reference crucible. The sample is heated with a constant heat rate until the desired temperature. The equipment used for the analysis is SETERAM TGA92 model.

In the case of SBA-15 samples, the mass variation is due to the water absorbed loss and the template decomposition, oxidation occurs under air atmosphere. The samples impregnated were analyzed in order to confirm the amount of CaO impregnated into the support. On the other hand, CaO-sorbents were analyzed under nitrogen atmosphere, and it is observed a mass loss because of the possible amount of hydroxides that can be present in the sample, occurring around the temperature of 400 ºC.

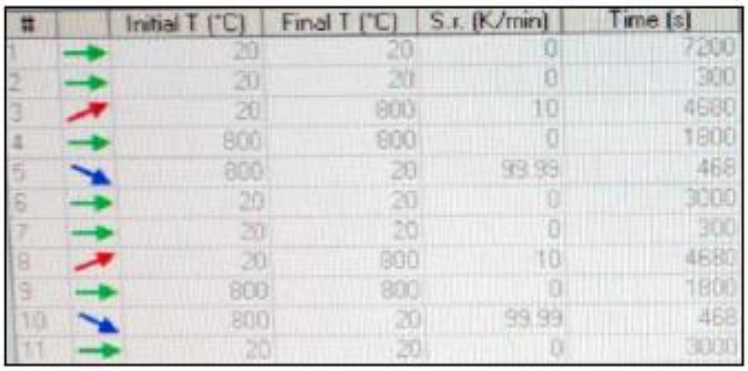

#		Initial T (°C)	Final T (°C)	S.r. (K/min)	Time (s)
1	→	20	20	0	7200
2	→	20	20	0	300
3	↗	20	800	10	4680
4	→	800	800	0	1800
5	↘	800	20	99.99	468
6	→	20	20	0	3000
7	→	20	20	0	300
8	↗	20	800	10	4680
9	→	800	800	0	1800
10	↘	800	20	99.99	468
11	→	20	20	0	3000

Figure 24: Defined program for TGA

3.4.2 X-Ray Diffraction (XRD)

X-Ray Diffraction is a technique mainly used for phase identification of a crystalline material. The material analyzed has to be finely milled and homogenized before it is placed onto a sample holder and introduced in the diffractometer. The XRD patterns were obtained in a Bruker D8 Advance X-ray diffractometer system, using a Cu Kα radiation and operating at 40 kV and 40 mA.

In order to identify the structure of the mesoporous samples, the 2θ angle range used was 0.7-5º, and the data were collected with a step size of 0.03º and a step time of 4s. In order to obtained about CaO-based samples, an angle range of 15-70º was used, with a step size of 0.03º and a step time of 4s.

3.4.3 Nitrogen sorption measurements

Isotherms analysis by physical adsorption is a method for obtaining information about the textural properties of porous material, such as surface area and pore size. According to IUPAC, adsorption isotherms are classified into six groups, depending on their shape (34) (35):

- **Type I:** it is also known as Langmuir isotherm. This type is characteristic in chemisorption and in physical adsorption only for microporous materials. It has a concave shape in P/P_0 axis and the amount absorbed achieves a limiting value (plateau) when $P/P_0 \rightarrow 1$, observing micropore filling and high uptakes at very low pressures.
- **Type II:** this type is typical for nonporous solids, where monolayer -multilayer adsorption occurs. At the beginning, the curve has a linear part and then it is transformed in a concave shape until an inflection point (called point B), which indicates that monolayer coverage is complete and multilayer adsorption starts to occur. At higher pressures, the curve in convex to the P/P_0 axis.

- **Type III:** this isotherm is convex to the abscissa axis over its entire range, indicating that the attractive interaction between adsorbate and adsorbent is weaker than in type II. These isotherms are not very common.
- **Type IV:** these isotherms are typical of mesoporous materials. The most characteristic feature of this type is the hysteresis loop, indicating that pore condensation occurs. The maximum uptake observed at high relative pressures shows a complete pore filling. The initial part has the same shape as in type II, which can be also assigned to monolayer-multilayer adsorption.
- **Type V:** although this type shows pore condensation and hysteresis as in type IV, the difference is that the first part of the isotherm has the same shape of type III, indicating the weak attractive interactions between the adsorbent and the adsorbate.
- **Type VI:** this particular isotherm represents the stepwise multilayer adsorption on a uniform, nonporous surface. The homogeneity of sorbent surface, the adsorptive and the temperature define the size of the steps.

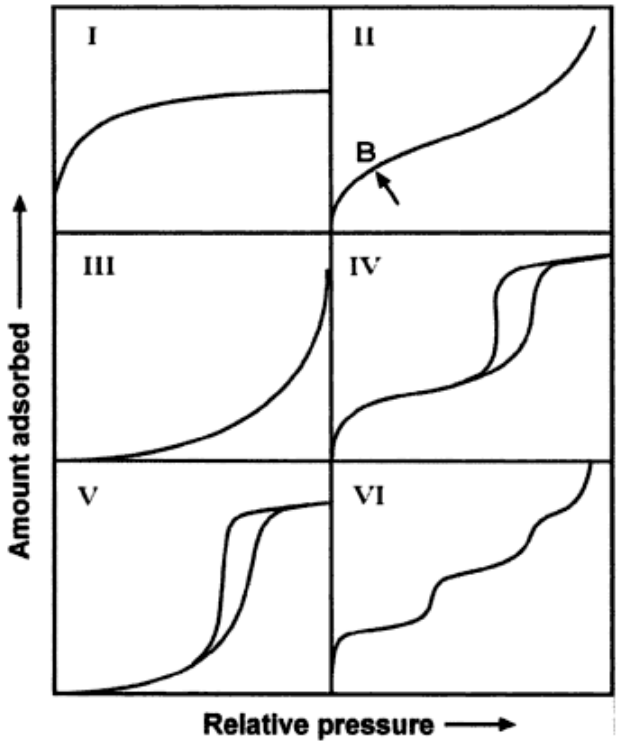

Figure 25: Adsorption isotherms clasiffication (35)

The sorption behaviour in mesopores solids depends on the fluid-wall attraction and on the interactions between the fluid molecules. For that reason, multilayer adsorption and capillary condensation are possible. A consequence of the capillary condensation is the apparition of the phenomenon called hysteresis, which can be shown in the type IV and V isotherms, where the adsorption and desorption curves do not coincide, obtaining the same amount adsorbed at two different relative pressure values (36).

According to IUPAC, the classification of the types of hysteresis is shown in figure 23, where: the first type H1 corresponds to mesoporous materials with cylindrical-like pore channels of well-defined diameter; type H2 corresponds to heterogeneous pores systems with network effects; type H3 is associated with non-rigid aggregates of plate-like particles; and the last type H4 corresponds to narrow slit pores, observed in micro-mesoporous materials (35) (36).

Mesoporous materials normally present isotherms of type IV with a hysteresis loop of type H1, indicating the presence of uniform cylindrical pores.

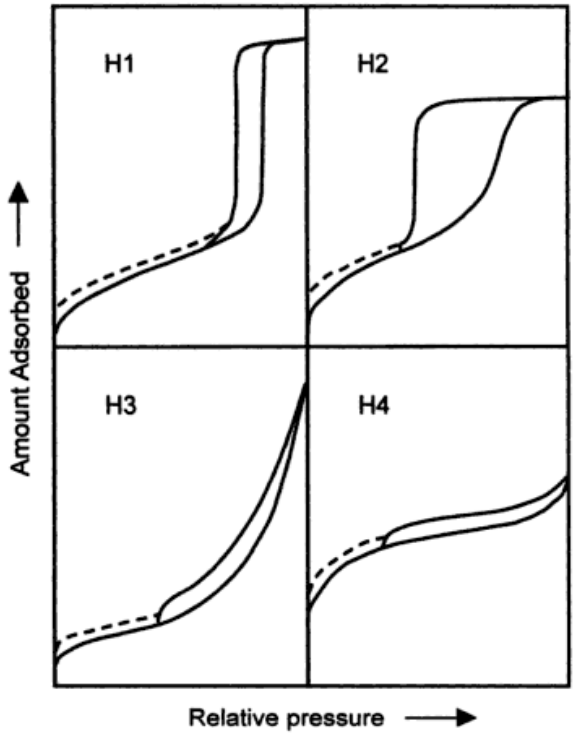

Figure 26: Hysteresis loops classification (35)

Kelvin equation is used with pores with uniform shape and width. This equation connects the pore diameter and the pore condensation pressure, and is the basis for the *Barett-Joyner-Halenda method* (BJH method), which is used in the mesopore analysis. For cylindrical pores, the modified Kelvin equation is used:

$$ln\frac{P}{P_0} = -\frac{2\gamma cos\theta}{RT\Delta\rho(r_p - t_c)} \quad \text{[eq. 5]}$$

in where: R is the universal gas constant; r_p is the pore radius; and t_c is the thickness of an absorbed multilayer film (36).

Brunauer, Emmett and Teller Model (BET)

The BET model was purposed in 1938 and is based on the Langmuir kinetic model. The first assumption considered is that multilayer adsorption is possible. The Van der Waals forces change in a different way, being stronger on the surface of the adsorbent than the forces between molecules of the gas phase, which are responsible of chemisorption. The adsorption forces are higher in the first layer and constant for the subsequent layers, for that reason the adsorption heat is superior in the first layer than in the others, because the first one is in contact with the adsorbent surface.

With these main considerations, it is possible to obtain the BET model equation, which has the following linear form (36):

$$\frac{{}^{P}/_{P_0}}{n(1-{}^{P}/_{P_0})} = \frac{1}{n_m C} + \frac{C-1}{n_m C}({}^{P}/_{P_0}) \qquad \text{[eq. 6]}$$

Where: n represents the adsorbed amount of gas at relative pressure; n_m is the amount of gas (adsorbate) required for monolayer coverage of the adsorbent (is also known as monolayer capacity); P is the equilibrium pressure of the gas and P_0 represents the saturated vapour pressure of the gas at the adsorption temperature; and C is the equilibrium constant of adsorption, which can be calculated with the following equation:

$$C = exp\left(\frac{Q_1 Q_L}{RT}\right) \qquad \text{[eq. 7]}$$

In eq. 7, Q_1 represents the heat of adsorption in the first adsorbed layer, and Q_L is the condensation heat. This equation allows the estimation of Q_1 knowing the experimental value of the constant C.

For mesoporous materials, the BET isotherm is applied in the relative pressure range from 0.05 to 0.3. In this way, the inclusion of adsorption data due to the volume filling of micropores and capillary condensation are avoided.

BET equation can be used in isotherms of type II or IV for the calculation of monolayer capacity n_m. It is necessary to represent $\frac{{}^{P}/_{P_0}}{n\left(1-{}^{P}/_{P_0}\right)}$ vs. ${}^{P}/_{P_0}$. With this representation, a slope (*m*) and an intercept (*b*) are obtained and reordering the terms of the parameters, it is possible to calculate the value of n_m and C, with the following expressions:

$$n_m = \frac{1}{m+b} \qquad \text{[eq. 8]}$$

$$C = \frac{m}{b} + 1 \qquad \text{[eq. 9]}$$

The surface area of the mesoporous solid can be obtained when the value of the monolayer capacity is known:

$$S_{BET} = N_A \cdot n_m \cdot \sigma_m \qquad \text{[eq. 10]}$$

Where:

N_A = Avogadro constant (6.022×10^{23})

n_m = monolayer capacity

σ_m = area occupied for each molecule of the monolayer (16.5 $Å^2$)

The analyses were carried out in an automatic Micrometrics ASAP 2010 apparatus. Prior the adsorption analysis, it is necessary to remove the water of the sample. For that, the sample is degased under vacuum at 90 ºC during 1 hour and subsequently at 300 ºC during at least 4 hours, assuring the complete degassing of the sample.

4 LAB-SCALE CO_2 CAPTURE UNIT

In this chapter, a description of the lab-scale CO_2 capture unit is presented, as well as the different steps in the carbonation-calcination cycles carried out in the reactor.

4.1 General description

The CO_2 capture unit is mainly formed by the following elements:

- **Fixed bed reactor:** it is made in quartz due to its resistance at high temperatures used in the cycling process (700-800ºC). The sorbent is supported by a porous plate. The reactor has an entrance for the thermocouple which measures the temperature in the fixed bed during the reaction, close to the sample.

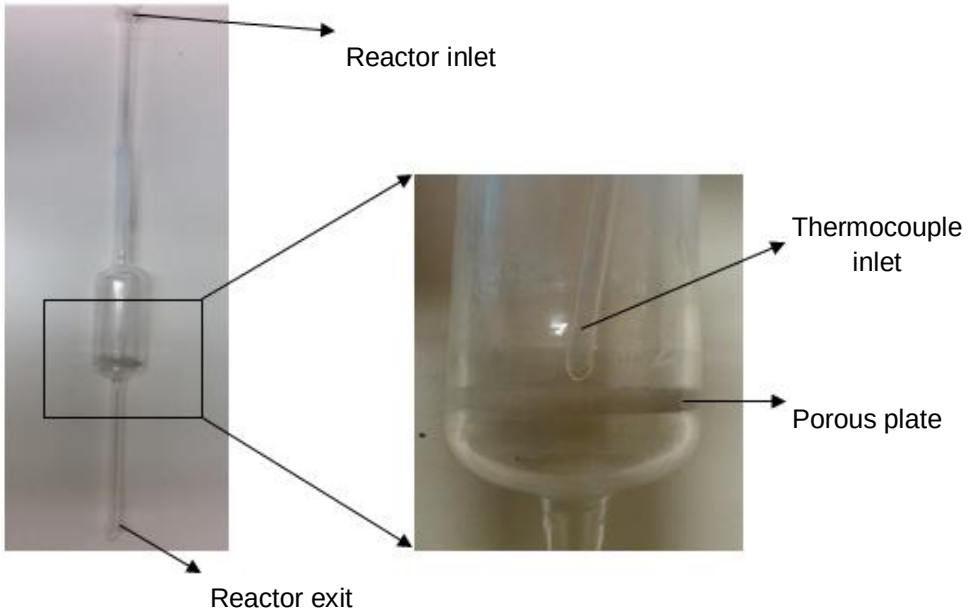

Figure 27: Fixed bed reactor scheme

- **Ceramic Oven:** it is composed by a controller which allows the temperature regulation in the process as well as the heating rate.
- **CO_2 Detector:** this detector performs the CO_2 concentration analysis at the reactor exit. The CO_2 detector produces a signal (4-20 mA) which is monitored and recorded with LabView software. The detector is a Guardian Plus 97350 model.
- **N_2 and CO_2 flowmeters:** allowing the control and regulation of the different CO_2 and N_2 flows that enter in the reactor.

In the next figure, a scheme of the CO_2 capture unit can be seen:

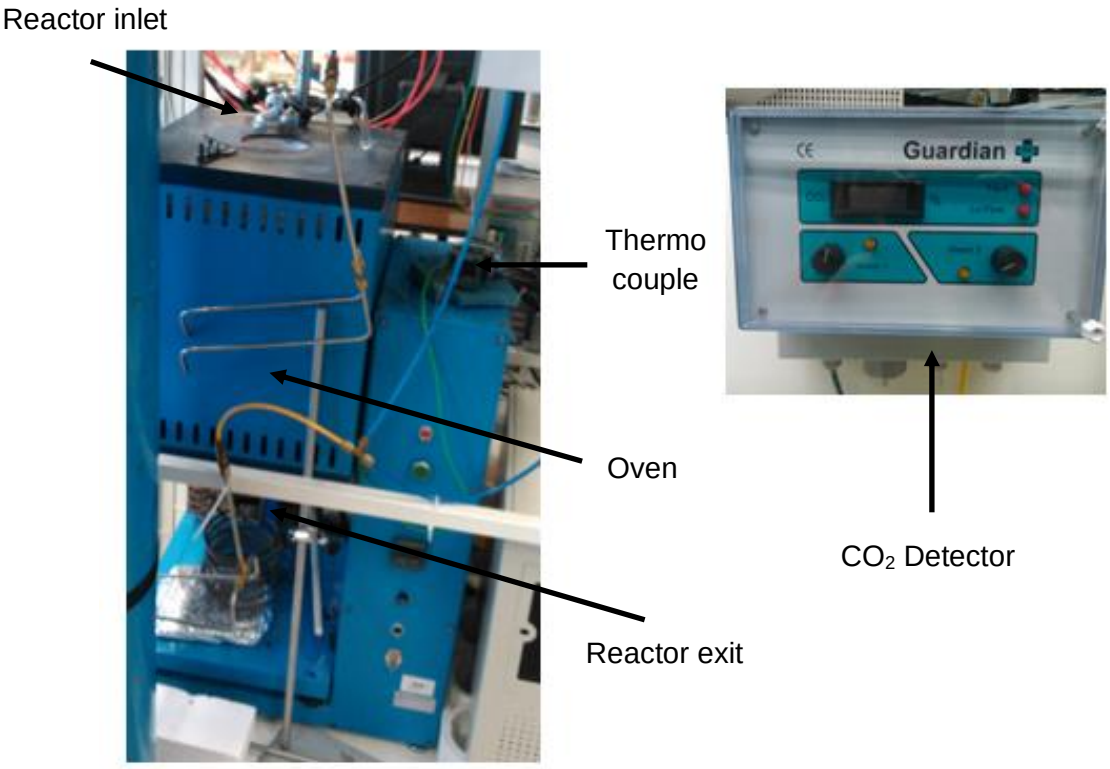

Figure 28: Lab-scale CO_2 capture unit

4.2 Experimental methodology

4.2.1 Detector calibration

Before running the experiment in the CO_2 capture unit, it is necessary to perform the calibration of the CO_2 detector. Several steps have to be followed:

1. Introduction of the empty reactor (without sorbent) in the unit oven,
2. Plug in the N_2 and CO_2 controllers and CO_2 detector,
3. Open the feed valves: N_2 and CO_2,
4. Define the desired N_2 flow and verify that there is not any gas leak on the entrance and exit of the reactor, using a bubble leak detector for gases called "*1000 bulles*",
5. Connect the software, producing immediately the record of the CO_2 concentration signal with the different positions of the CO_2 valve for the calibration,
6. After the end of step 5, stop the program and, when CO_2 detector indicates 0.00%, close the N_2 and CO_2 flows and gas valves.
7. Determine the calibration curve (slope and intercept), which represents the signal produced vs. the CO_2 concentration measured.

4.2.2 Reactor unit startup

After the calibration, the next step the reactor loading with the desired sorbent and the startup of the reactor unit.

1. Weight the desired sample and introduce it in the reactor, which is hold in a support plate. It is important that the sample stays in a uniform way over the porous plate,
2. Introduction of the reactor with the thermocouple in the oven,
3. Connection of the N_2 and CO_2 controllers, CO_2 detector, and the temperature switch,
4. Open the feed valves: N_2 and CO_2,
5. Define the desired N_2 flow and verify that there is not any gas leak in the entrance and exit of the reactor, using the leak detector for gases called "*1000 bulles*",
6. Define the position desired for the CO_2 detector valve.
7. Connect the software, using the slope and intercept data got in the calibration process,
8. Put the set point at 800ºC and switch on the oven,

The carbonation-calcination cycles start, following the next procedure:

1. The reactor is heated until 800ºC, with only the N_2 valve opened,
2. When the temperature is reached, the first calcination takes place during 1 minute, decreasing the temperature subsequently until 700ºC.
3. At 700ºC, the CO_2 valve is opened and the carbonation stage occurs during 5 minutes,
4. After that, the CO_2 valve is closed and the temperature is increased until 800ºC again, finishing the carbonation reaction,
5. At that temperature, calcination reaction takes place during 10 minutes
6. Then, temperature is decreased again, beginning a new cycle.

When all cycles are concluded, the set point is changed to 20ºC in order to cool down the reactor. After that, the N_2 and CO_2 flow valves are closed, and the CO_2 detector and the oven are turned off.

5 EXPERIMENTAL RESULTS

In this chapter, all experimental results obtained are presented and divided in several sections. The first section explains the influence of the different experimental parameters involved in the synthesis of SBA-15, comparing different methods and different experimental conditions.
Secondly, it is carried out a study about the thermal stability of SBA-15 calcined at different temperatures, with all corresponding characterization. The next section presents the part of impregnation process with the calcium source, and the subsequent study of thermal stability of the samples. Then, samples were tested in the CO_2 capture unit and the results are presented in section number four. Finally, in the last section is explained the results obtained of some experiments tested in the lab-scale CO_2 capture unit, using CaO synthetic sorbents with different characteristics of synthesis.

5.1 Synthesis of SBA-15 materials

In this section, the objective is to compare two different synthesis methods (conventional and microwave-assisted synthesis) and also different experimental conditions and their influence in the final properties of the materials obtained. First, the two different synthesis methods, explained in the previous chapters, are compared. Then, some experimental parameters were also modified during microwave-assisted synthesis, and their influence in the final properties were studied. All the materials were calcined at 550 ºC under the same thermal conditions. The table 5 summarizes the different conditions used for the synthesis of the materials.

Table 5: Synthesis conditions of SBA-15 samples

SAMPLE	TEOS PRE-HYDROLYSIS TEMPERATURE / DURATION	HYDROTHERMAL TREATMENT SYNTHESIS METHOD
S_CL	40 ºC / 2h	Conventional 100ºC / 48h
S_MW	40 ºC / 2h	Microwave 170ºC / 2h
S_MW_140_1	40ºC / 4h	Microwave 140ºC / 1h
S_MW_140_2	40ºC / 4h	Microwave 140ºC / 2h
S_MW_170_1	40ºC / 4h	Microwave 170ºC / 1h
S_MW_170_2	40ºC / 4h	Microwave 170ºC / 2h

* All samples were synthesized with the **molar ratio: 1 SiO_2 : 0.02 P123 : 6.33 HCl : 178 H_2O**

5.1.1 Influence of synthesis method

The first two samples (S_CL and S_MW) were synthesized under the same conditions: the P123 was first dissolved into an acid solution at 40ºC during 4h and then the pre-hydrolysis of TEOS was carried out also at 40ºC during 2h. The crystallization treatment was subsequent done under conventional or microwave heating, during 48 and 1-2 h respectively.

XRD patterns of the first two as-synthesized materials are displayed the next figure 29. It can be seen that whatever the heating method used, three well-defined peaks were detected in both samples, corresponding to (100), (110) and (200) reflections characteristics of highly ordered hexagonal structure of SBA-15.

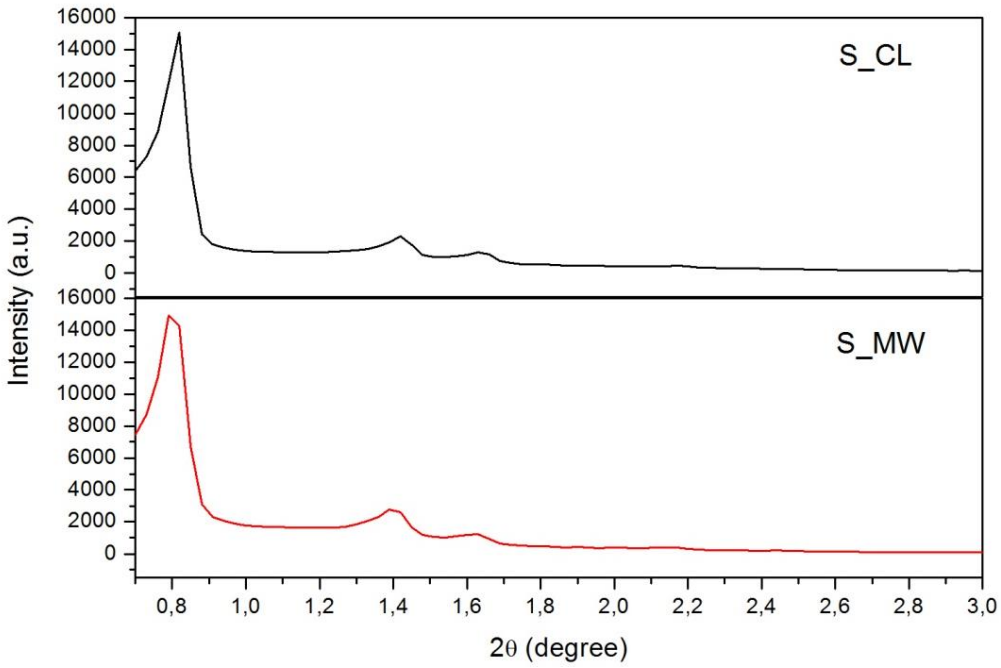

Figure 29: X-Ray diffraction patterns for SBA-15 samples synthesized by conventional and microwave-assisted method

Nitrogen sorption isotherms of the corresponding samples are reported in figure 30 and it can be seen that both correspond with isotherms type IV and hysteresis loop H1, typical of well-ordered mesoporous materials, which is well in line with XRD results. The isotherm inflection point of the material synthesized under conventional heating is slightly moved to lower relative pressures, indicating a smaller pore size in the material. The plateau ordinate is also higher, meaning that pore volume is increased with comparing with MW synthesized material. Also, one can see that MW sample possesses a lower surface area (slope between 0,05 and 0,3 P/P_0) and less micropores than the conventional sample. One explanation might be a higher silica condensation under MW conditions, and consequently the disappearance of some surface area and micropores, confirming the study of *Jaroniec et al* (27). The textural parameters extracted from isotherms are presented in table 6. The pore size distribution (PSD) of both samples is shown in figure 31. Conventional sample shows a

maximum at about 78 Å while MW sample shows larger pores (85 Å). Following *Jaroniec et al* (27), the use of microwave radiation during SBA-15 crystallization can provoke a partial decomposition of P123 template and a swallowing of the respective pores.

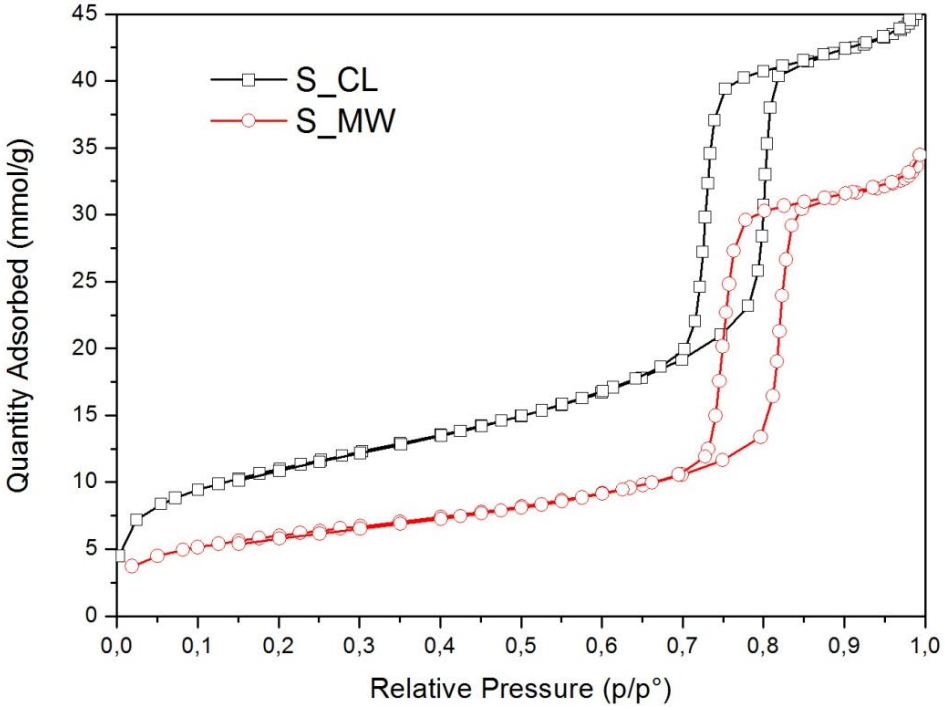

Figure 30: N_2 sorption isotherms of SBA-15 samples synthesized by conventional and microwave-assisted method

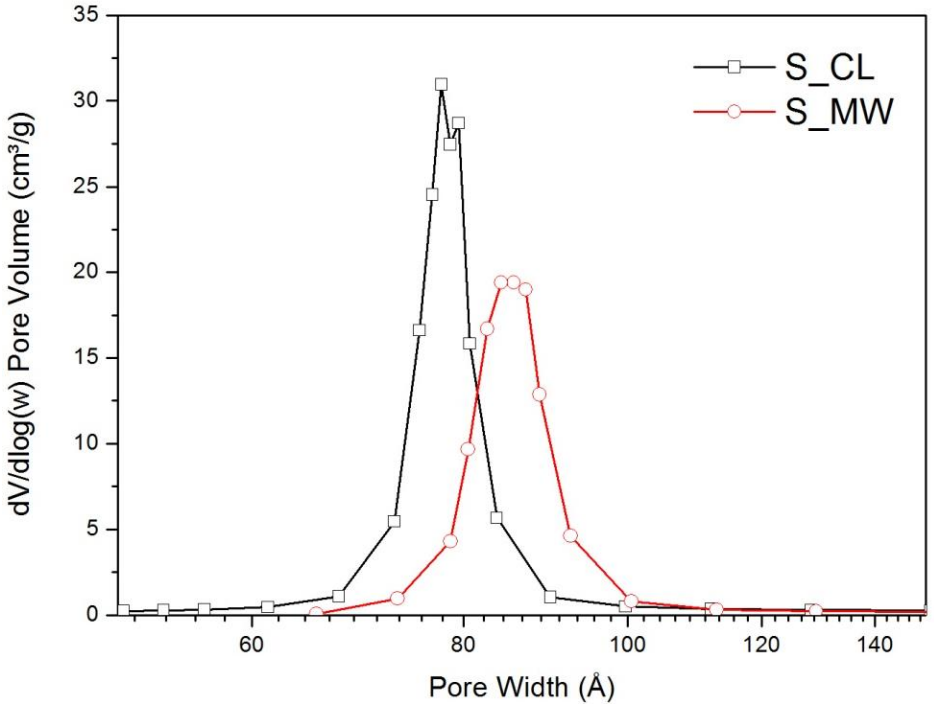

Figure 31: PSD of SBA-15 samples synthesized by conventional and microwave-assisted method

5.1.2 Influence of experimental parameters in hydrothermal treatment

In the second part of this study, some experimental parameters were modified in order to study the optimal conditions for the synthesis of SBA-15 using microwave radiation. The parameters studied were temperature and crystallization time, as well as the duration of TEOS pre-hydrolysis. Temperature and crystallization time were 140 and 170 ºC and 1 or 2 hours, respectively. The temperature in the pre-hydrolysis step (TEOS + template solution) was 40ºC and was maintained fixed in all samples. Concerning the duration of TEOS pre-hydrolysis, times of 2 or 4 hours were used. The experimental conditions of the synthesized samples can be seen in table 5, displayed above.

First, the influence of the experimental conditions in the hydrothermal treatment using microwave radiation is presented. Small-angle ray-diffractions analysis was made in order to know if the structure of mesoporous materials changed with the modification of the synthesis parameters. Figure 32 confirms that all samples present a hexagonal ordered structure characteristic of mesoporous materials. The three well-defined peaks were detected. However, it seems that higher crystallization temperature or time favors more crystalline materials as XRD peaks increase in intensity with the increase of the former parameters.

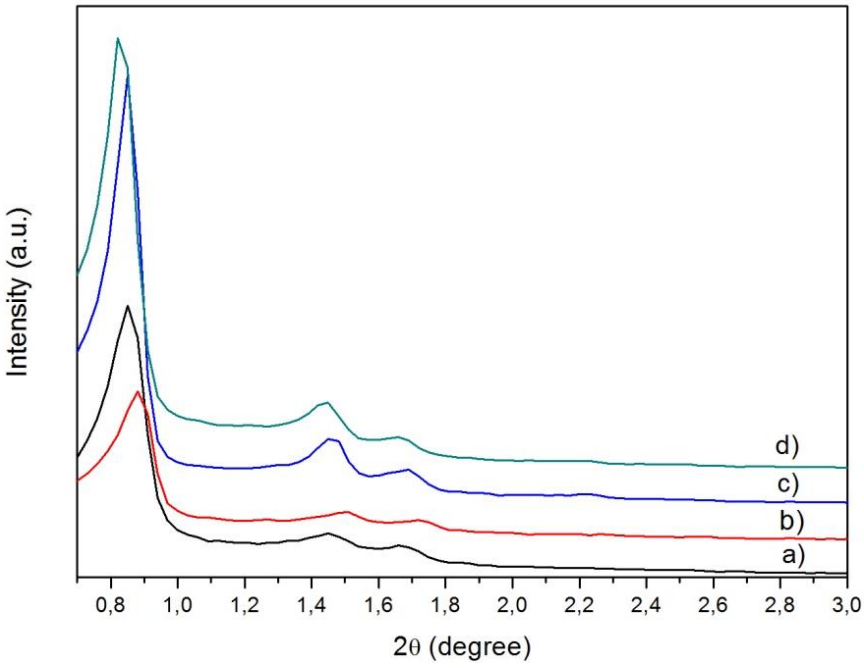

Figure 32: X-Ray diffraction patterns for SBA-15 samples synthesized by microwave at different temperatures and times: a) S_MW_140_1; b) S_MW_140_2; c) S_MW_170_1; d) S_MW_170_2

In figure 33, N_2 adsorption/desorption isotherm curves for all samples are presented. The textural parameters calculated from those curves are collected in table 6. All samples present isotherms of type IV with a H1 hysteresis loop. The inflection point shifts gradually to higher relative pressures when temperature is increased, at the same time the height of the capillary condensation

range also increases with temperature). These results show that mesoporous materials with uniform pores are obtained when crystallization temperature and time are increased, conforming XRD results.

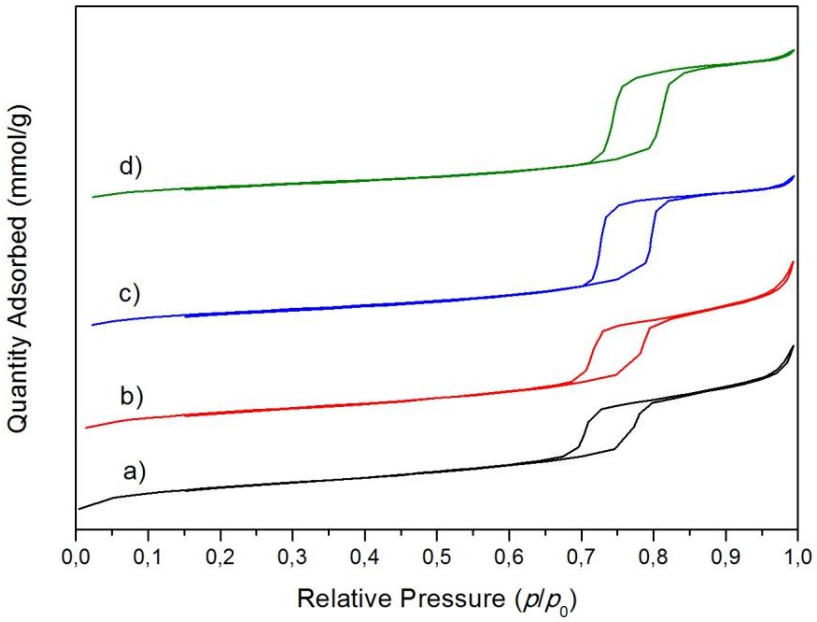

Figure 33: N2 sorption isotherms of SBA-15 samples synthesized by microwave at different temperatures and times: a) S_MW_140_1; b) S_MW_140_2; c) S_MW_170_1; d) S_MW_170_2

The pore size distribution curves are shown in figure 34. It can be seen that samples synthesized at lower temperature show a broader distribution when are compared with high temperature synthesized samples, confirming the good pores size homogeneity of samples synthesized at 170 ºC. Also, the intensity of the peaks corresponding to S-MW-140 samples is lower, which means that they present less pores volume (see table 6).

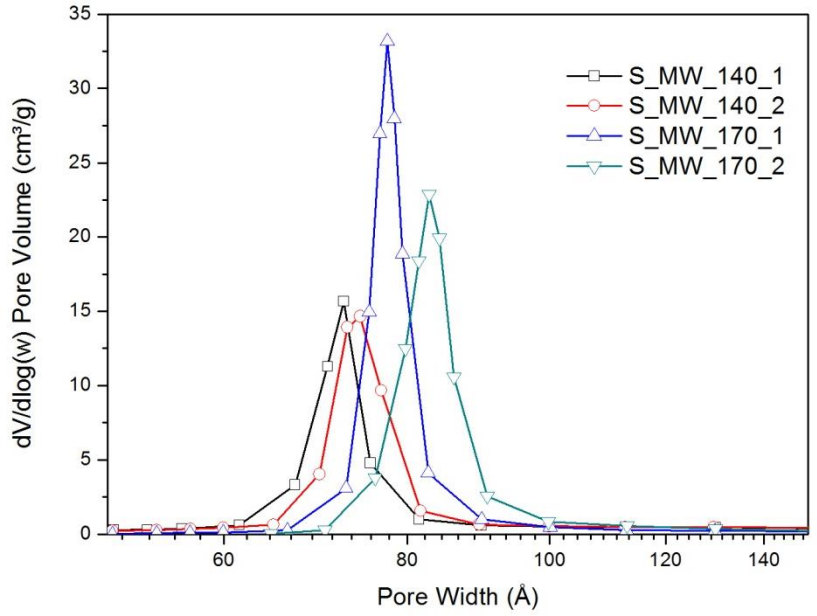

Figure 34: Pore size distribution of SBA-15 samples synthesized by microwave at different temperatures and times

5.1.3 Influence of time in pre-hydrolysis step

In order to study the influence of the time in the TEOS pre-hydrolysis step, two SBA-15 samples were compared: one with 2 hours of duration (S_MW) and the other, with 4 hours (S_MW_170_2). Both samples were synthesized using microwave conditions at 170 ºC during 2 hours. The XRD diffractograms obtained are compared in figure 35. The three peaks are observed for both samples, indicative of highly ordered mesoporous structures. However, in the case of the samples synthesized with 2 hours, the peaks are more intense.

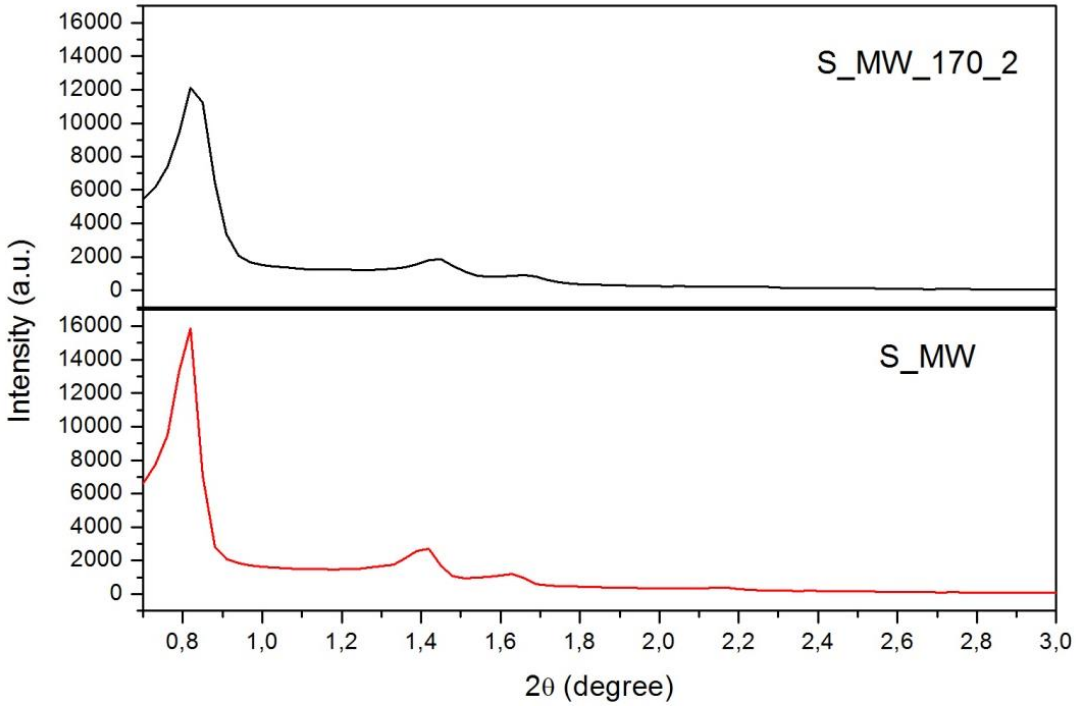

Figure 35: X-Ray diffraction patterns for SBA-15 samples synthesized by microwave at different pre-hydrolysis time

The figure 36 shows the isotherms obtained for samples S_MW and S_MW_170_2. Both samples show isotherms of type IV, although S_MW presents a profile better defined. In fact, in the figure 37 where PSD are presented, one can see that S_MW shows a sharper peak with pores of smaller size. However, from the table 6, it can be seen that textural parameters for each samples are rather similar.

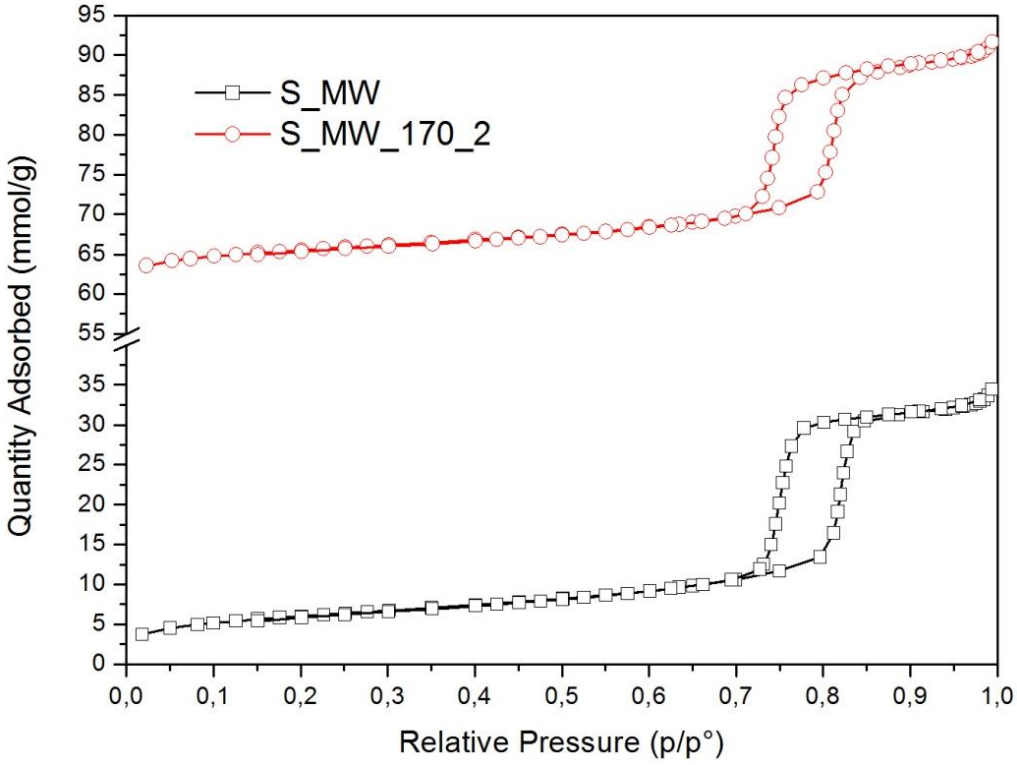

Figure 36: N2 sorption isotherms of SBA-15 samples synthesized by microwave at different pre-hydrolysis time

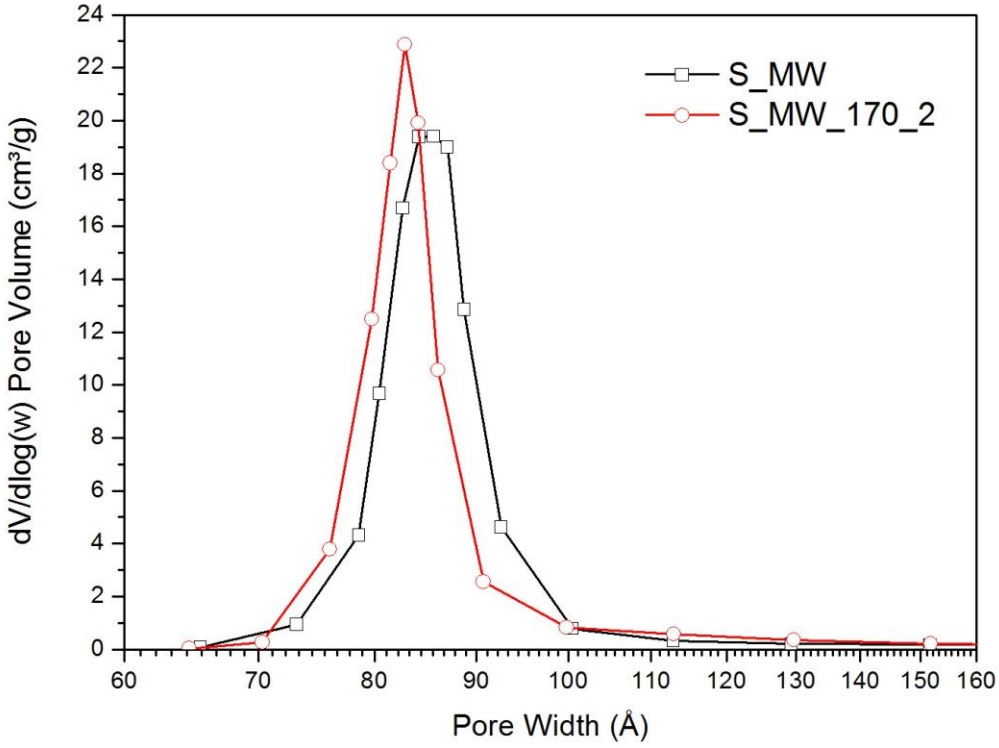

Figure 37: PSD of SBA-15 samples synthesized by microwave at different pre-hydrolysis time

The table 6 shows the textural parameters derived from N_2 sorption isotherms, obtained for all samples.

Table 6: Textural properties of SBA-15 samples synthesized

SAMPLE	S_{BET} (m^2/g)	$V_{micropore}$ (cm^3/g)	$V_{mesopore}$ (cm^3/g)	D_{BJH} (Å)
S_CL	884	0.11	1.19	78
S_MW	484	0.05	0.92	85
S_MW_140_1	662	0.05	0.58	72
S_MW_140_2	605	0.04	0.58	74
S_MW_170_1	522	0.03	0.84	78
S_MW_170_2	450	0.03	0.84	80

The results obtained in this section can be compared with the study carried out by *Jaroniec et al.* (27), where several SBA-15 materials were synthesized with the help of microwave and under different conditions, during hydrothermal treatment: the range of temperature was 40-200 ºC and the range of crystallization time was 1-12 h. Conditions for the TEOS pre-hydrolysis step were 40 ºC during 2 hours. After that, they tested varying the duration of the stirring step from 1 h to 10 h. Results of their research suggest that the optimal conditions of crystallization step for SBA-15 synthesis under microwave method were high temperatures (between 160-180ºC) during 3-6 hours of crystallization time. Results of the present thesis confirm the optimal conditions observed above: samples with better structural and textural results were those synthesized at 170ºC during 1 and 2 hours. In the case of comparison of pre-hydrolysis step time, results were similar for both SBA-15 samples, confirming the optimal conditions used during this work. Nevertheless, it is important to emphasize that the results obtained with 4 hours of TEOS pre-hydrolysis step and in the case of 170ºC during 2h (sample S_MW_170_2), after filtering step, the sample presented a lightly yellowish colour instead of white colour. It could be because of degradation suffered in template during the hydrothermal process.

After analysing all the results obtained, it can be confirmed that the duration of TEOS pre-hydrolysis step does not seems to influence a lot the final materials properties. Consequently, in what follows, only the SBA-15 samples synthesized with 2 hours of pre-hydrolysis are considered.

5.2 Thermal stability of SBA-15 materials.

The aim of this section is studying the thermal stability oh samples calcined at different temperatures. Samples synthesized by conventional and microwave method (S_CL and S_MW), referred to in table 5 of section 5.1, were calcined at different temperatures: 700, 800 and 900 ºC. After that, the corresponding structural and textural characterization were made and the results compared with the samples calcined at 550 ºC.

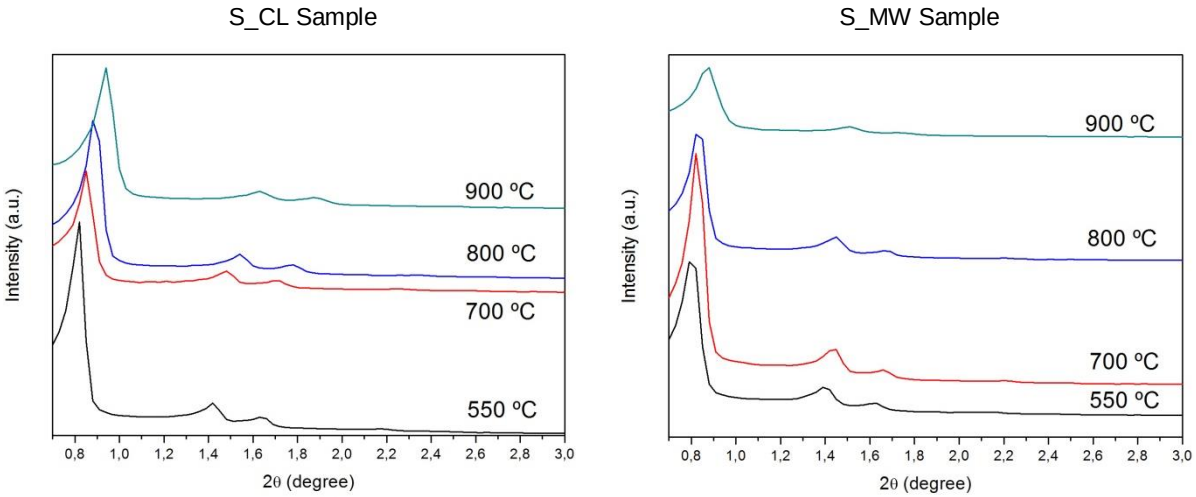

Figure 38: X-Ray diffraction of SBA-15 synthesized by conventional (left) and microwave method (right)

XRD patterns of the resulting materials are displayed in figure 38. The diffraction patterns show that the 2-D hexagonal ordered structure is maintained even after the calcination at 900ºC for both samples. The peaks are softly shifted to higher values of 2θ angles when the temperature of calcination increases, indicating that the mesoporous network suffers a small shrank (condensation) when samples are calcined at high temperatures.

Nitrogen sorption isotherms of the corresponding samples are reported in figure 39. It can be seen that all the sample present a type IV isotherm with a hysteresis loop H1, typical of mesoporous materials. For both synthesis methods (conventional and microwave), the isotherms are moved to lower relative pressures and lower amount of N_2 absorbed when the temperature of calcination is increased. This means that there is a reduction in the pore width and in the pore volume for both samples. However, these changes are stronger for samples synthesized under conventional conditions, while under microwave conditions only the decrease of N_2 adsorbed is more pronounced, as the condensation capillary happens rather at the same relative pressure.

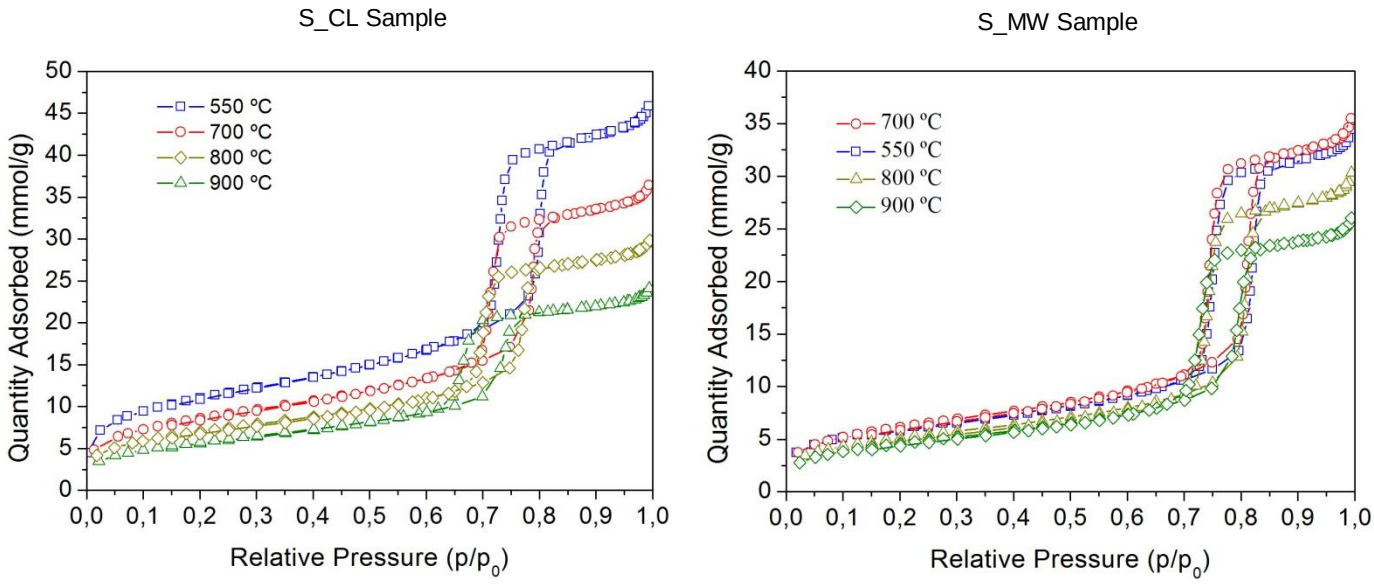

Figure 39: X-Ray diffraction of SBA-15 synthesized by conventional (left) and microwave method (right)

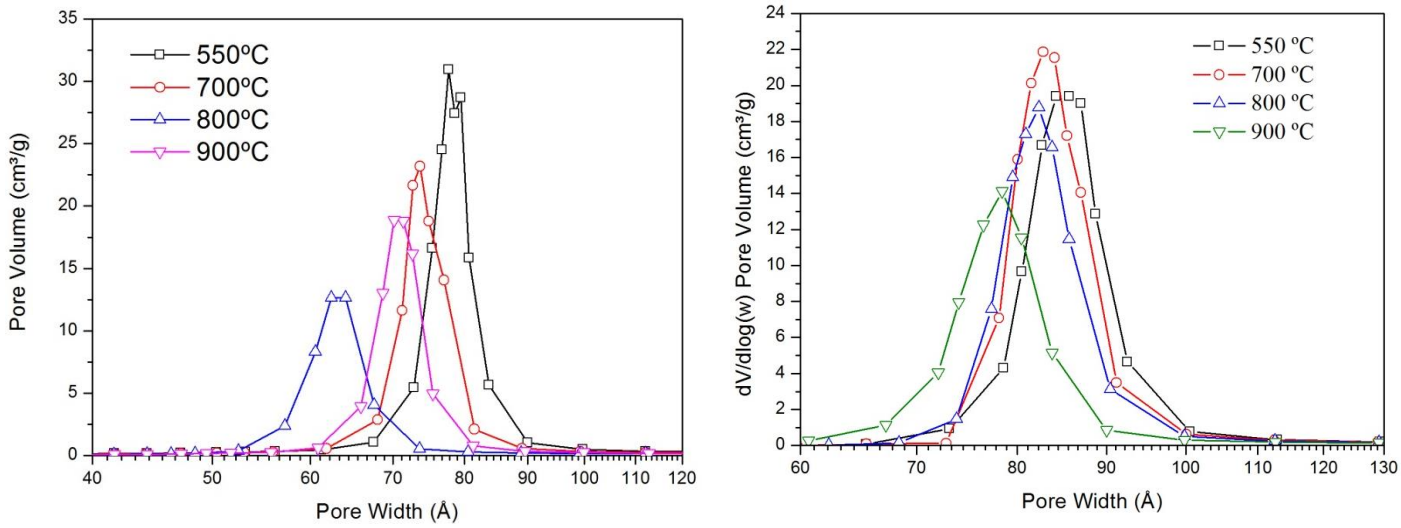

Figure 40: PSD curves of SBA-15 materials synthesized by conventional (left) and microwave (right) methods and calcined at 550, 700, 800 and 900 ºC

The figure 40 shows the PSD curves obtained for the two samples, as a function of calcination temperatures. In both cases, the PSD maxima shift to lower relative pressure, indicative of a reduction of pore size. The effect is more pronounced for conventional sample. At the same time, pores size distribution become broader, which is well in line the decrease of the XRD peaks and the fact that at relative high temperatures the mesoporous material starts to suffer irreversible structural and textural damages. Additionally, one can see that complementary micropores disappear with temperature, in both cases, as a direct consequence of pronounced condensation and subsequent structure destruction. In the table 7, the different textural values obtained for these materials calcined at different temperatures, are presented.

Table 7: Textural properties of calcined SBA-15 samples

SAMPLE	S_{BET} (m^2/g)	$V_{micropore}$ (cm^3/g)	$V_{mesopore}$ (cm^3/g)	D_{BJH} (Å)
S_CL 550ºC	884	0,11	1,19	78
S_CL 700ºC	698	0,05	0,98	73
S_CL 800ºC	573	0.03	0.81	70
S_CL 900ºC	472	0,02	0,63	63
S_MW 550ºC	484	0,05	0,92	85
S_MW 700ºC	501	0,05	0,95	80
S_MW 800ºC	418	0,03	0,80	82
S_MW 900ºC	377	0,03	0,70	79

In summary, it can be confirmed that samples synthesized by microwave method present more thermal stability than the other samples. In fact, from table 7, it can be seen that conventional samples rapidly loses surface area and pores volume, while microwave sample still present good textural parameters up to 700 ºC.

5.3 Stability study of Ca/SBA-15 samples

5.3.1 Impregnation of SBA-15

Once that SAB-15 samples thermal stability study was evaluate for different temperatures, the next step concerned the study of SBA-15 as support material for Ca-based materials used in the CO_2 capture. For that purpose, a new sample was synthesized using MW and optimized experimental conditions and subsequently impregnated.

After the results obtained above, the new sample was synthesized under microwave conditions in the hydrothermal treatment (170ºC during 2h). In the same way as that for the previous sample, the conditions were 40ºC during 4h for the P123 dissolution and 40ºC during 2h for the TEOS addition. The sample was characterized after the synthesis.

Table 8: Preparation conditions of the new support

SAMPLE	MOLAR RATIO	HYDROTHERMAL TREATMENT SYNTHESIS METHOD
S_MW2	1 SiO_2 : 0.02 P123 : 6.35 HCl : 178.79 H_2O	Microwave 170ºC / 2h

The calcium source used in the impregnation was calcium nitrate tetrahydrate ($Ca(NO_3)_2 \cdot 4H_2O$). In fact, among the different Ca sources, calcium nitrate is well soluble in water (~1293 g/L H_2O at 20ºC) and can easily decompose after calcinations, to form CaO, making easy the preparation of Ca-based materials. In order to achieve samples with 10% and 20% Ca in weight with respect SBA-15 support, the following conditions were used:

Table 9: Preparation of SBA15-Impregnated Ca samples

SAMPLE	SBA-15 *(g)*	$Ca(NO_3)_2$ *(g)*	Ca-wt% theoretical
S_MW_10Ca	2.00	1.26	10%
S_MW_20Ca	2.00	2.95	20%

After impregnation and subsequent calcination, Ca/SBA-15 samples were characterized with the purpose of evaluating the physicochemical properties of the resultant materials. Figure 41 shows the thermogravimetric analysis performed for both samples impregnated, before calcination at 550ºC.

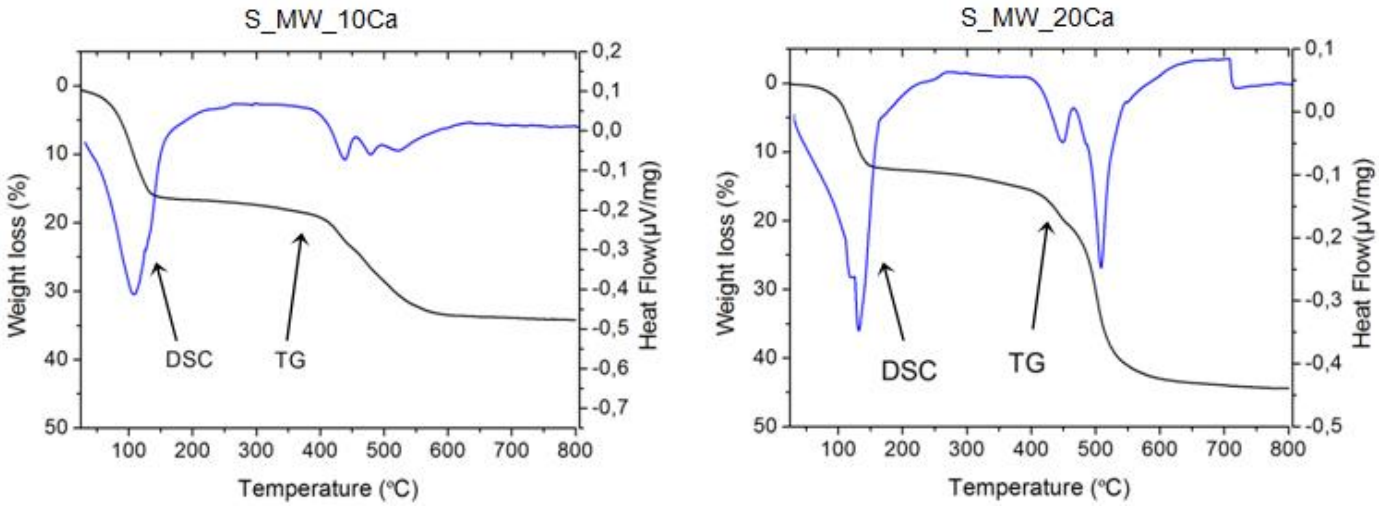

Figure 41: TG and DSC curves of S_MW_10Ca (left) and S_MW_20Ca (right).
DSC curve corresponds to left axis and TG curve yo right axis.

For the two samples, the weight losses are decomposed in two steps: the first one can be attributed to the loss of water physically absorbed (endothermic peak around 100ºC); the second one corresponds to the decomposition of $Ca(NO_3)_2$. The second step presents two peaks between 400 and 600ºC. In sample with 10 wt-% Ca, the amount of water lost corresponds to 16.5% while for the second sample, the amount is about 12.4%. These high values can be explained by the fact that samples were placed into the saturator before experiment. The amount of weight loss corresponding to nitrate decomposition is about 17.6 and 32.1% for the two samples, respectively. It can be seen that the heat peaks in sample with 20 wt-% Ca are higher, when are compared with S_MW_10Ca and occur at slightly higher temperatures. This is normal because the sample requires more energy for the decompositions due to the higher amount of calcium nitrate.

The XRD patterns are presented in the following figure 42. It can be seen that all samples show an intense peak, characteristic of large pores present in the materials. However, only raw material and S_MW_10Ca sample show the two additional peakss, meaning that these two samples show 2D-hexagonal structure. Probably S_MW_20Ca lost this 2D-hexagonal organization because of the important amount of Ca nitrate during the impregnation preparation. The intensity of the peaks for Ca-impregnated samples decreases with the increase of Ca amount. This is probably due to the decrease of electronic density contrast between pore walls and the inner pore, with the introduction of Ca metal oxides.

XRD experiments at high angles were also carried out in order to detect other phase coming from the addition of Ca during the impregnation. The results are shown in figure 42 (inset). No extra peak characteristic of CaO phase was found. It can be concluded that: a) CaO particles are too small so they do not produce any diffraction peak, i.e. CaO phase is well dispersed in the SBA-15 material; b) Ca reacted with support silica, producing an amorphous phase, not detectable by XRD technique.

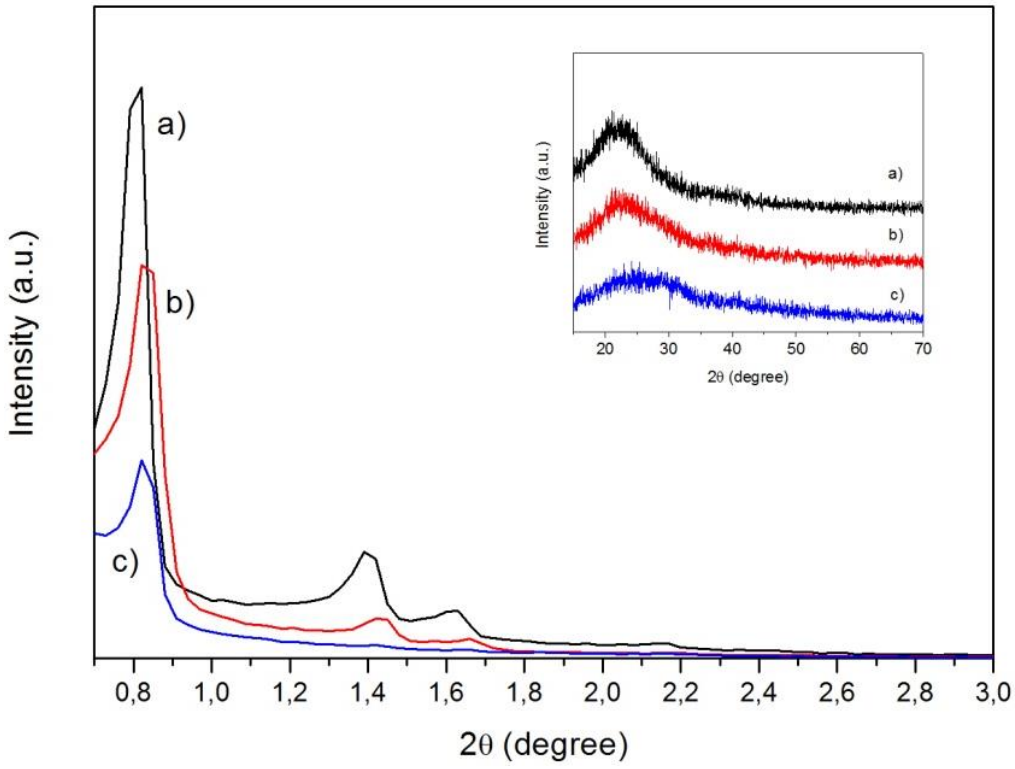

Figure 42: Small and high-angles XRD patterns of Ca/SBA-15 samples: a) raw; b) 10 wt-% Ca; c) 20 wt-% Ca

The nitrogen sorption isotherms and the pore size distribution of the samples are represented in figure 43 and 44. The isotherm of S_MW2 sample presents the typical isotherm of mesoporous materials: type IV with a H1 hysteresis loop. The isotherm of the sample with 10 wt-% Ca has also the same aspect as the S_MW2, which means that S_MW_10Ca sample maintained the ordered mesoporous structure, although with a shift for lower amount of N_2 adsorbed, which means that Ca species are covering the surface of the mesopores. In the case of sample with 20 wt-% Ca, the amount of N_2 also decreases, however, the capillary condensation step is moved to higher pressures, probably because some structural transformation occurs, i.e. Ca impregnated reacts in some way with the mesoporous silica, leading to an amorphous material with a somewhat different porous system, i.e. higher pores size.

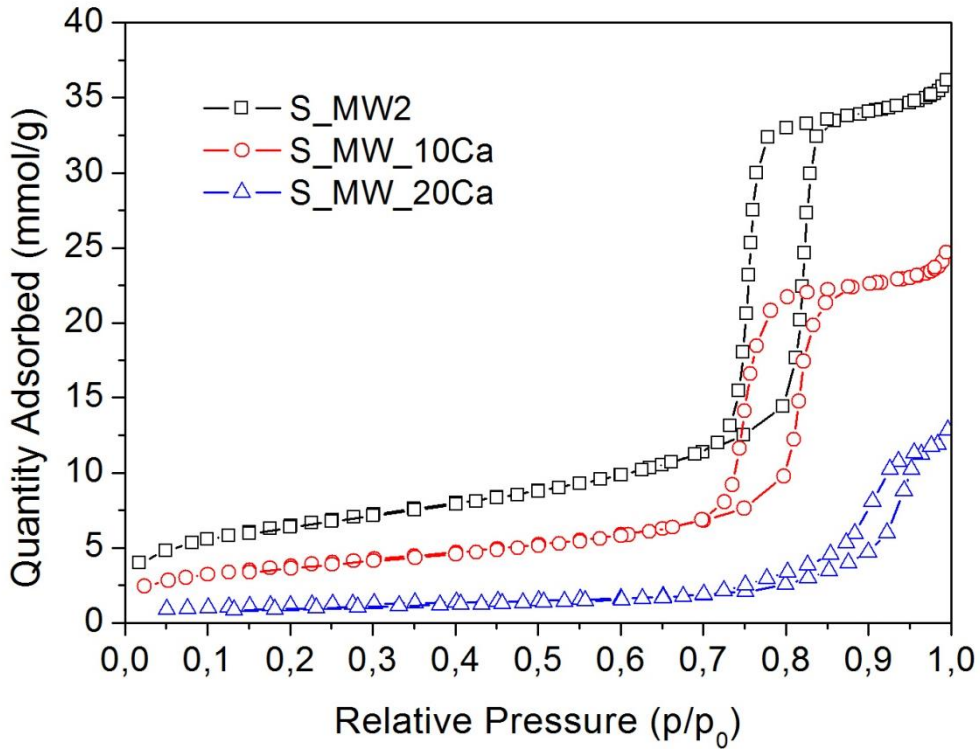

Figure 43: N_2 adsorption/desorption isotherms of Ca/SBA-15 (0-10-20 wt-% Ca)

The PSD curves obtained for the three different materials are presented in figure 43 and illustrate well the comments from the previous paragraph. Textural properties of these three samples are also collected in table 10.

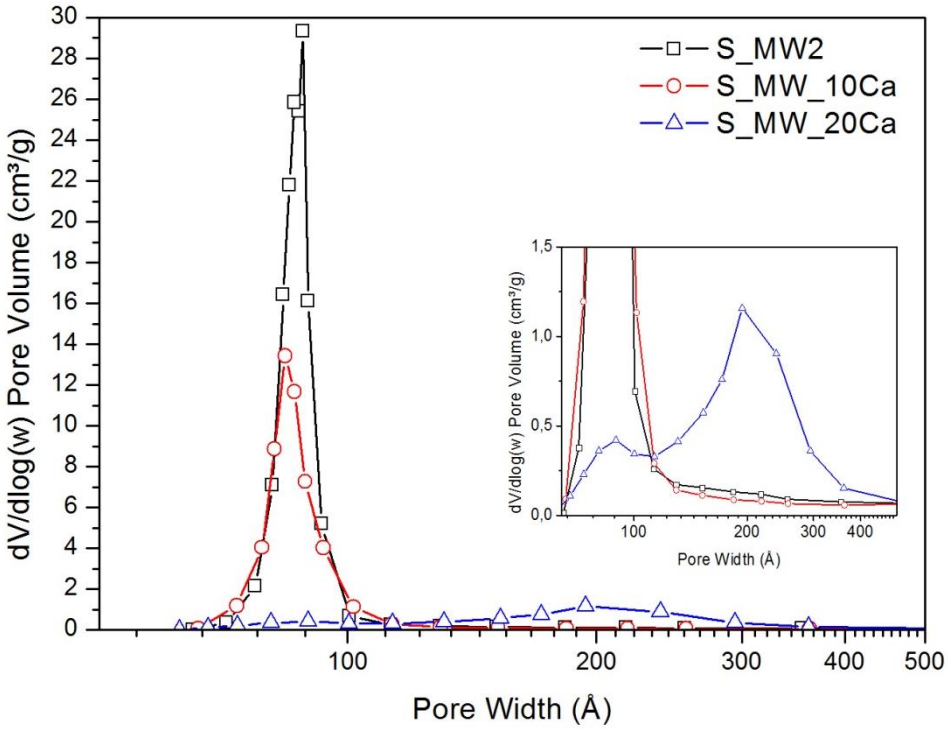

Figure 44: Pore size distribution curves of Ca/SBA-15 (0-10-20 wt-% Ca)

5.3.2 Thermal stability study of Ca/SBA-15

With the objective of using the Ca/SBA-15 synthesized samples in the CO_2 capture experiments, it is necessary to study the stability of Ca-based SBA-15 materials under similar conditions as for the CO_2 looping cycles experiments. As it has been explained in the literature review (Chapter 2), the CO_2 capture process carried out in a lab scale unit is formed by several repeated cycles at high temperatures: 700 and 800ºC. So that, it is important to know if the mesoporous structure can thermally tolerate such high temperature calcinations/carbonations repetitions. In this way, both Ca/SBA-15 samples were subjected to a blank test with 10 cycles under an inert atmosphere (only nitrogen, without carbon dioxide). After that, all corresponding characterizations were realized in order to study the structural and textural stability of the samples.

From X-ray diffraction analysis (figure 45), it can be seen that in both samples the typical 2-D hexagonal ordered structure of mesoporous materials is rather maintained. In the case of S_MW_10Ca, the three peaks corresponding at (100), (110) and (200) planes can be observed, although the two later are very weak in intensity, which means that structure starts to collapse. This happening is even more obvious for S_MW_20Ca where only the first peak (100) is observable. High-angle XRD patterns also presented in figure 45, show that no characteristic peak from CaO phase can be detected. For the sample S_MW_10Ca, there is a peak detected at value 2θ = 38.5º but it corresponds to the sample-holder used.

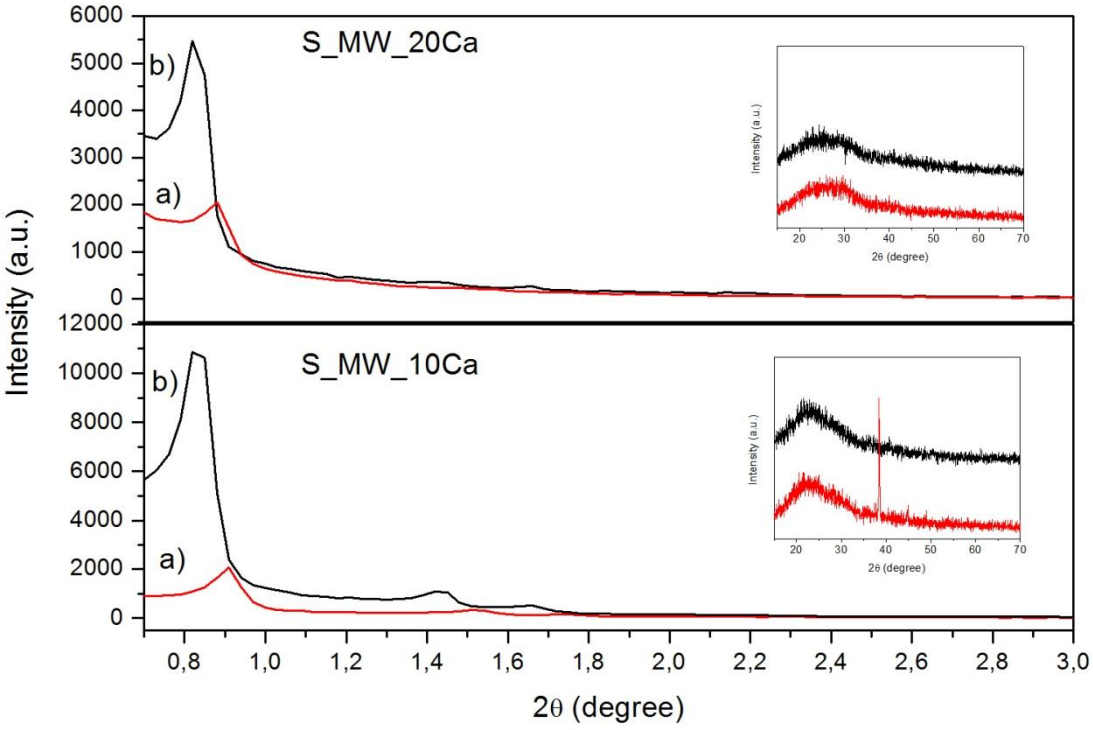

Figure 45: Small and high-angle XRD of S_MW_10Ca and S_MW_20Ca a) before and b) after blank test

N_2 sorption analysis was done for both samples after the blank test and the results were compared with the previously one obtained before test. The N_2 isotherms and the pore size distributions of the samples are collected in figures 46 and 47. Concerning S_MW_10Ca (left graph) the isotherm obtained after blank test is substantially different, which can be interpreted as a rather significant structure transformation suffered by S_MW_10Ca sample. In fact, the isotherm presents a strongly modified hysteresis loop, which can be explained by the appearance of a non-uniform pores distribution. For the other sample S_MW_20Ca, the isotherm is very similar to the one observed before the blank test, meaning that in this specific case, no strong structural and textural changes occur.

These statements are confirmed with the respective pore size distribution curves, which are presented in figure 47. In the left figure (S_MW_10Ca samples), it can be seen that pores size distribution of the sample is strongly affected by the thermal treatment, as some pores with higher diameter (~100-200 Å) appear. For the other sample, pores still have bimodal distribution with pores having size 91 and 203 Å, the latter being the major contribution. The textural parameters obtained are summarized in the table 10.

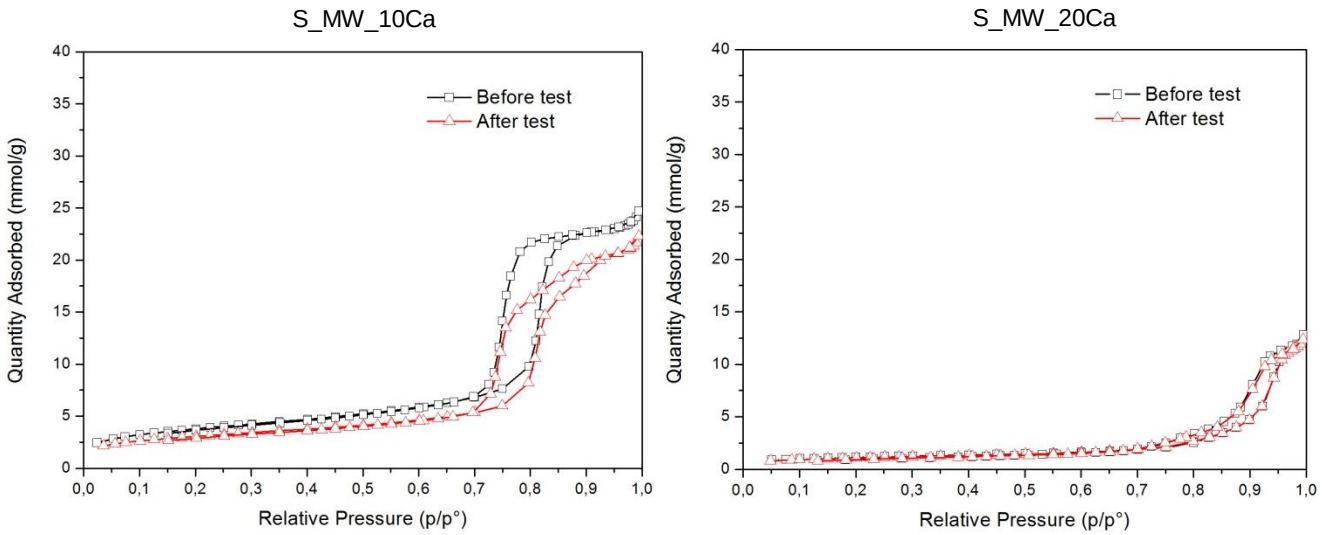

Figure 46: N_2 adsorption/desorption isotherms of S_MW_10Ca (left) and S_MW_20Ca (right) before and after blank test

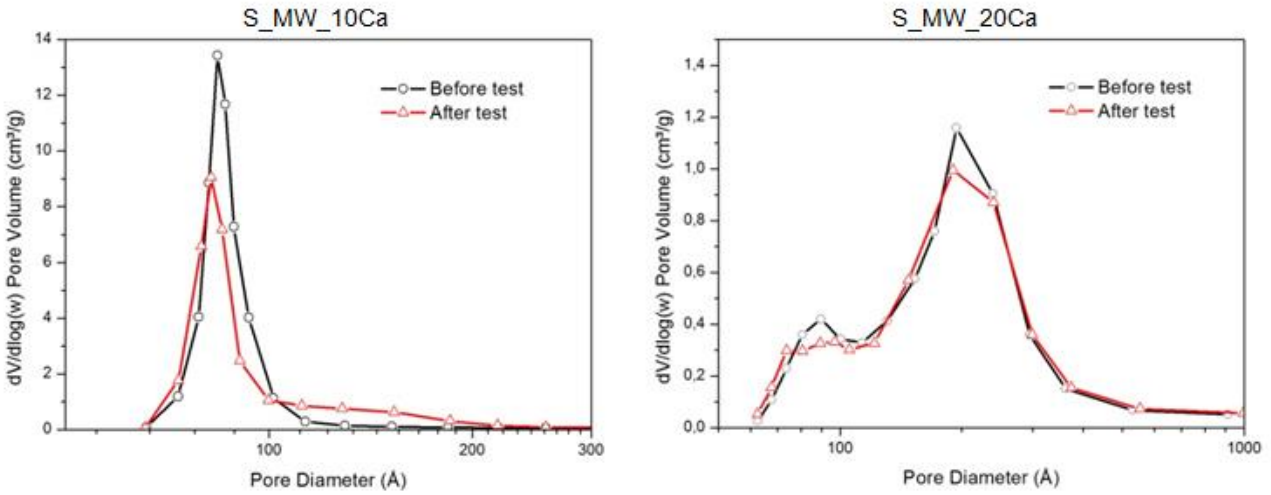

Figure 47: Pore size distribution curves of S_MW_10Ca (left) and S_MW_20Ca (right) before and after blank test

Table 10: Structural and textural properties of impregnated samples, before and after test

SAMPLE	S_{BET} (m^2/g)	$V_{micropores}$ (cm^3/g)	$V_{mesopores}$ (cm^3/g)	D_{BJH} (Å)	t (Å)
S_MW2	522	0.05	1.03	88	36
S_MW_10Ca	307	0.03	0.67	85	39
S_MW_20Ca	92	0.014	0.08	88/200	36
S_MW_10Ca after blank test	247	0.017	0.45	82	30
S_MW_20Ca after blank test	88	0.009	0.16	91/203	25

The results presented above show an important decrease in the textural values (surface area and pores volume) for the Ca-based SBA-15 materials prepared by impregnation, when compared with raw SBA-15 sample, especially when the amount of Ca os high (S_MW_20Ca). However, while significant structural transformations seem t happen to S_MW_10Ca samples during thermal blank test, leading to high differences in the final textural properties, no significant changes are observed for S_MW_20Ca sample.

5.4 Ca-based SBA-15 sorbents in carbonation-calcination cycles

After evaluating the thermal stability of Ca/SBA-15, the next step was the evaluation of their capacity to be used in CO_2 capture, i.e. their capacity in adsorbing CO_2 during calcinations-carbonations cycles. Samples S_MW_10Ca and S_MW_20Ca were used hereafter.

5.4.1 Lab-scale CO_2 capture unit

In order to determine the carrying capacity of the SBA-15 samples impregnated with calcium, experiments with 10 cycles were carried out in the lab-scale CO_2 capture unit, with the following conditions used in each cycle:

- *Carbonation:* 5 minutes of duration at 700ºC under a mixed flow composed by 15%CO_2 (v/v) (corresponding with 143.6 ml/min) and 850 ml/min of N_2.
- *Calcination:* 10 minutes of duration at 800ºC under a pure flow of 850 ml/min of nitrogen.

In figure 48, it is shown the typical profile of CO_2 concentration along the cycles which is obtained by the data acquisition LabView software connected to the CO_2 detector.

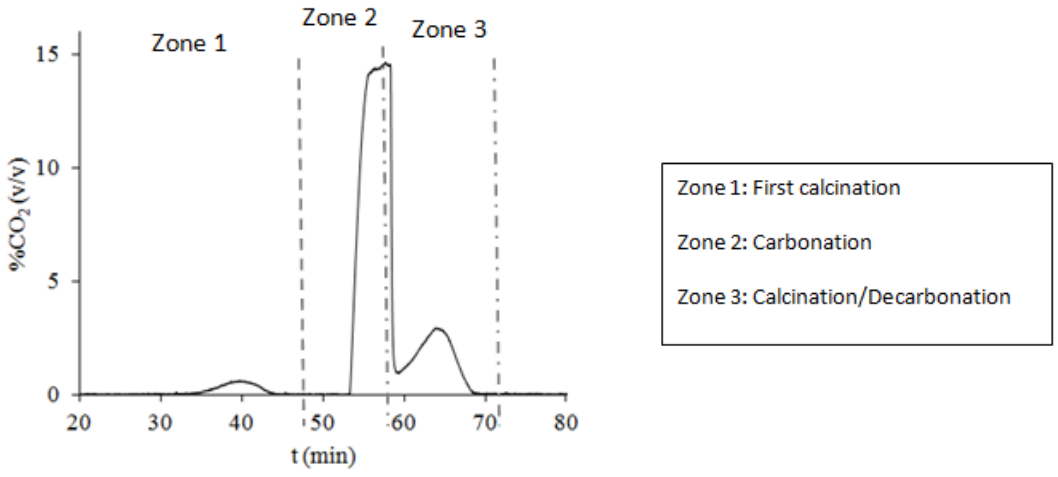

Figure 48: Typical CO_2 concentration profile along one cycle acquired with LabView software

Unfortunately, in our present study, no amount of CO_2 adsorbed in the CaO samples could be detected. Figure 49 shows the profile of CO_2 concentration obtained in the test with S_MW_10Ca sorbent. It can be seen that only the CO_2 release for the first calcination (zone 1) is detected. Zone 3 does not appear, which indicates that only a very low not detectable amount of CO_2 was adsorbed by the Ca-based SBA-15 samples. This can be probably due to the small amount of calcium into the samples that makes the CO_2 release too low to be detected by the CO_2 detector. For S_MW_20Ca sample, the same profile was obtained, meaning that higher amounts of Ca are most likely needed during impregnation step. Due to time constraints, it was not possible to prepare impregnated sorbents increasing the amount of calcium in order to obtain good results during the CO_2 capture experiments.

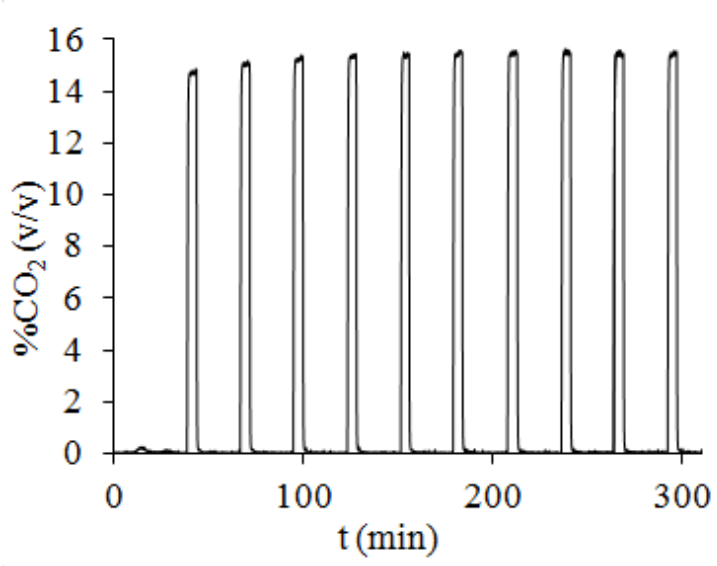

Figure 49: CO_2 concentration profile along the time acquired with LabView software in S_MW_10Ca sorbent.

Nevertheless, S_MW_10Ca sample was characterized after the test in the CO_2 capture unit. The sample maintains the hexagonal structure of ordered mesoporous (figure 50). However, the N_2 isotherm obtained for that sample is very different when comparing with either S_MW_10 or S_MW_10Ca after blank test. In figures 51 and 52, N_2 sorption isotherms and pore size distributions are presented. The isotherm obtained after the test with CO_2 presents a modified hysteresis loop characteristic of a non-uniform pore distribution and is quite different when comparing with S_MW_10Ca after blank test. It means that, although no CO_2 capture is observed because of detector limitations, CO_2 seems to have a certain impact on the final textural properties of the material. It seems that CO_2 accelerates the phenomenon observed during blank test, as now PSD curve is wider and shows the application of only pores with higher diameter (117 Å). The different textural parameters can be seen in table 11.

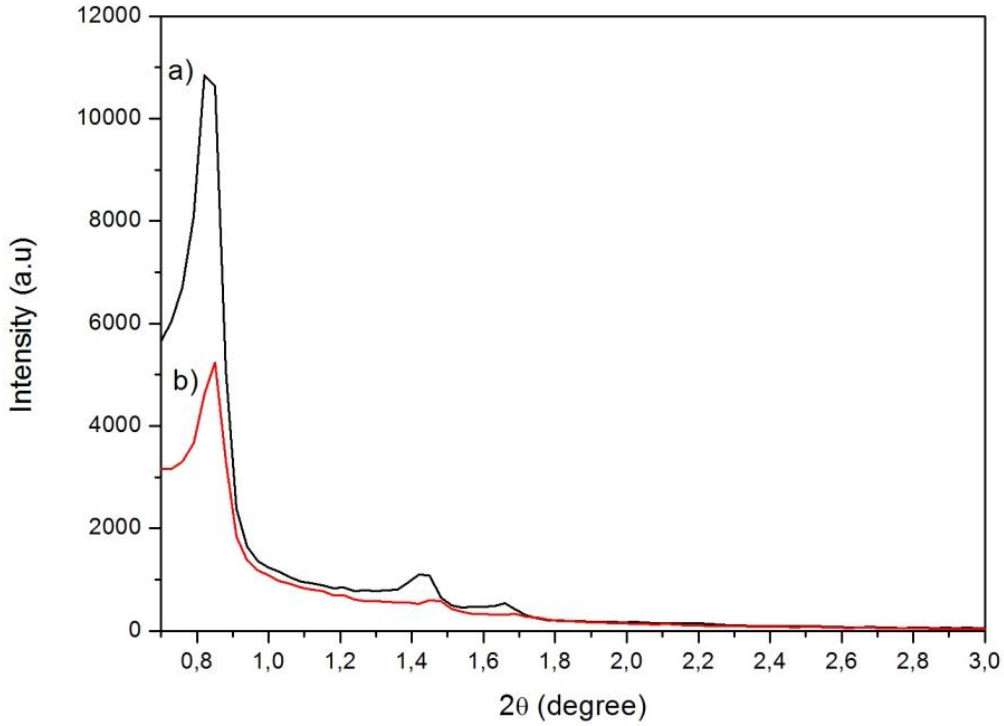

Figure 50: Small-angle XRD of S_MW_10Ca a) before and b) after CO_2 capture test

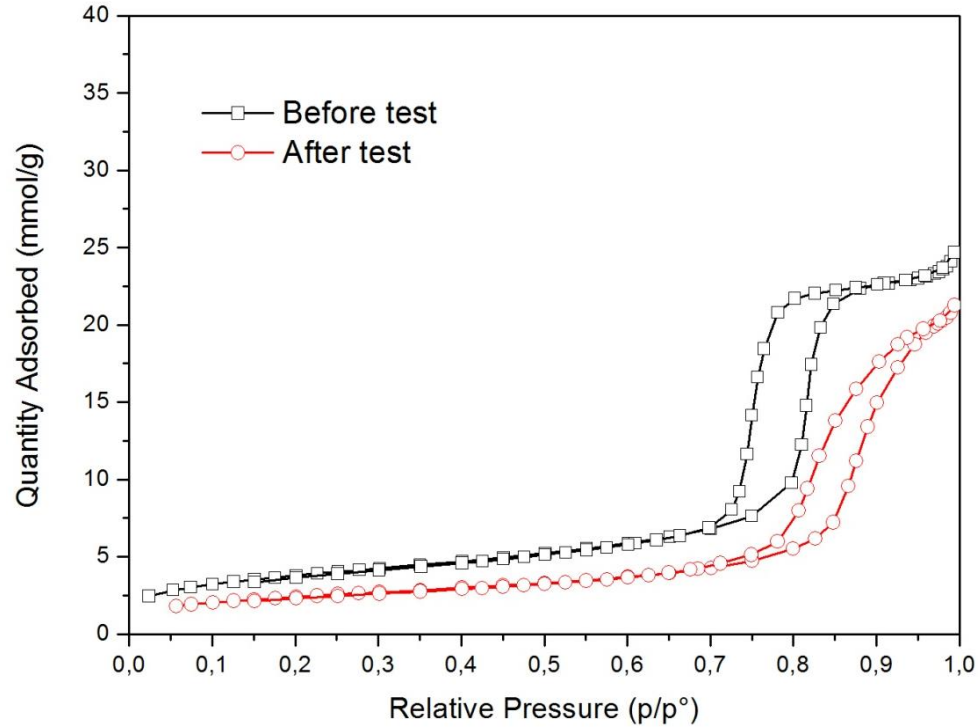

Figure 51: N_2 adsorption/desorption isotherms of S_MW_10Ca before and after CO_2 capture test

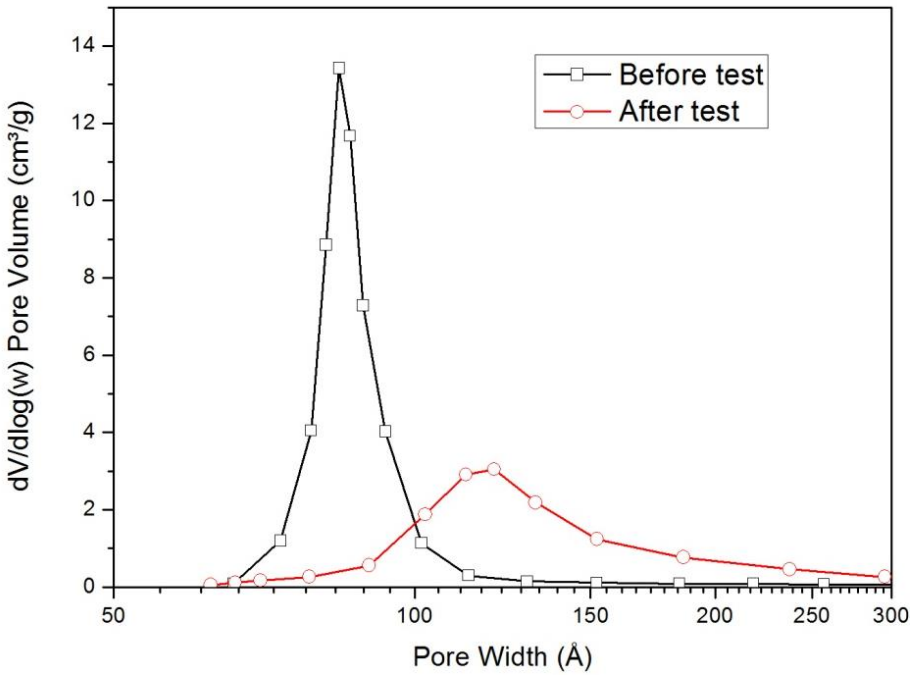

Figure 52: Pore size distribution curves of S_MW_10Ca before and after CO_2 capture test

Table 11: Structural and textural properties of S_MW_10Ca before and after CO_2 capture test

SAMPLE	S_{BET} (m^2/g)	$V_{micropores}$ (cm^3/g)	$V_{mesopores}$ (cm^3/g)	D_{BJH} (Å)
S_MW_10Ca	307	0.03	0.67	85
S_MW_10Ca after CO2 capture	197	0.01	0.43	117

5.4.2 Thermogravimetric analysis

The CO_2 capture tests were also performed by the means of thermogravimetric analysis, in order to evaluate the CO_2 capture capacity of Ca-based SBA-15 samples. Figure 53 shows the typical temperature profile during *n* cycles used in TG experiments. Calcination was carried out at 800 ºC under a pure flow of N_2 (30 mL/min) during 17 min, and carbonation step was performed at 700 ºC under 15%v/v of CO_2 for a total volumetric flow rate of 30mL/min with N_2 balance, during 48 min.

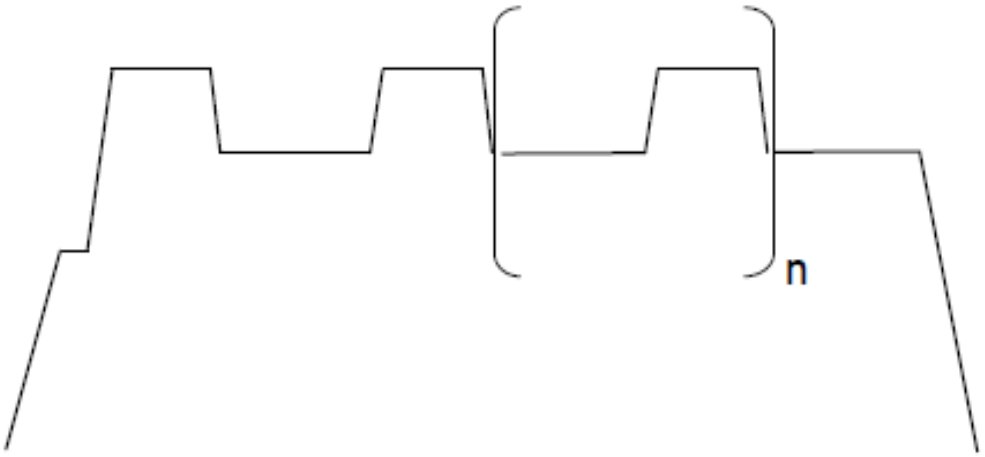

Figure 53: Typical temperature profile during carbonation-calcination cycles in the TG unit

First, S_MW_20Ca sample was tested, using a sample mass of 21.12 mg that corresponds theoretically to 5.91 mg of CaO sorbent. In figure 54, the temporal evolution of the loss mass and the temperature are shown. It can be observed the loss mass of the sample during the first calcination, followed by an increase in the mass during CO_2 adsorption (carbonation reaction), and then the release of CO_2 during the calcination step.

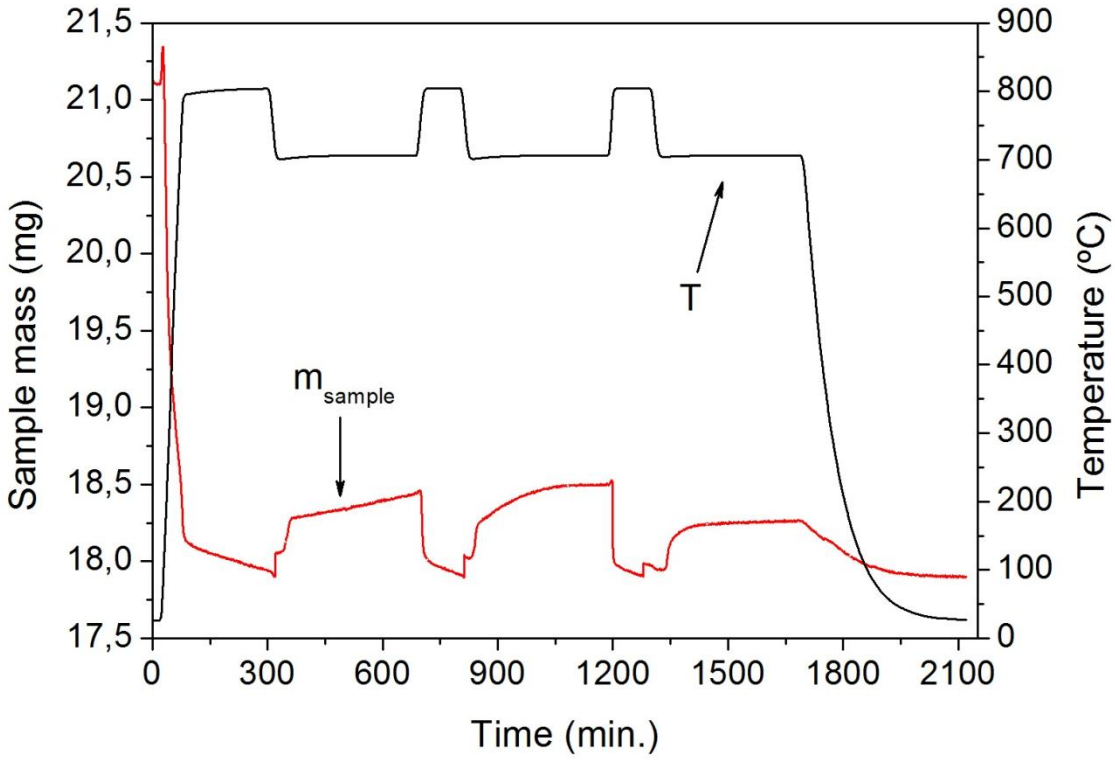

Figure 54: Temporal evolution of the sample mass and temperature for S_MW_20Ca

The S_MW_10Ca sample was tested under the same conditions in the TG unit. After the tests, the carrying capacity of the Ca/SBA-15 sorbents was calculated, in terms of g CO_2 / g CaO. In the next table, the different reactivity values obtained are presented.

Table 12: Carrying capacity of S_MW_10Ca and S_MW_20Ca

N cycles	S_MW_10Ca (g CO_2 / g CaO)	S_MW_20Ca (g CO_2 / g CaO)
1	0.08	0.11
2	0.08	0.13
3	0.09	0.07

Results show that the reactivity of both sorbents is very low, confirming that it is necessary impregnate more amount of calcium in the SBA-15 support in order to obtain higher reactivity. For the sample S_MW_20Ca, the values in the first and second cycle are practically similar, while in the third cycle the capacity decreases, probably because the sorbent starts to deactivate. On the other hand, S_MW_10Ca sorbent seems to be more stable and since it presents the same values in the three cycles.

5.5 Non-supported CaO sorbents

Following the results obtained by Joana Hipólito (20), three synthetic non-supported CaO sorbents were also prepared and studied in this work for a better understanding of the influence of the calcination temperature at the end of the preparation step, and also for comparing their CO_2 capture activity with that of the prepared Ca/SBA-15 supported sorbents.

The three CaO sorbents were synthesized by sol-gel method using the same conditions used by Joana Hipólito (20), only modifying the temperature of calcination at the end of the preparation step, and also using in one of the samples a different structurant in the preparation step. Carbonation-calcination cycles were carried out in the same conditions explained in the previous section, which are similar to the conditions used in the experiments of previous research work (20). Table 13 shows the structurants used in the preparations and the calcination temperature at the end of the preparations.

Table 13: Synthesis conditions of CaO sorbents

SAMPLE	STRUCTURANT	CALCINATION TEMPERATURE
CA_250_2	Activated Carbon (250 mg)	750ºC at 2ºC/min
CA_BP_250_2	Carbon BP2000 (250 mg)	750ºC at 2ºC/min
SG_2	-	750ºC at 2ºC/min

Figure 55 shows the results obtained for 10 cycles of carbonations and calcinations for the three sorbents prepared in this work calcined at 750 ºC in the preparation step, and also for the sorbent CA_250_2 850ºC previously prepared in Joana Hipólito work (20), where the calcination temperature used at the end of the preparation was 850 ºC. It is also possible to compare the results obtained with the different CaO-based sorbents using granular activated carbon and BP2000 as structurants in the sol-gel synthesis, with the sample prepared without structurant.

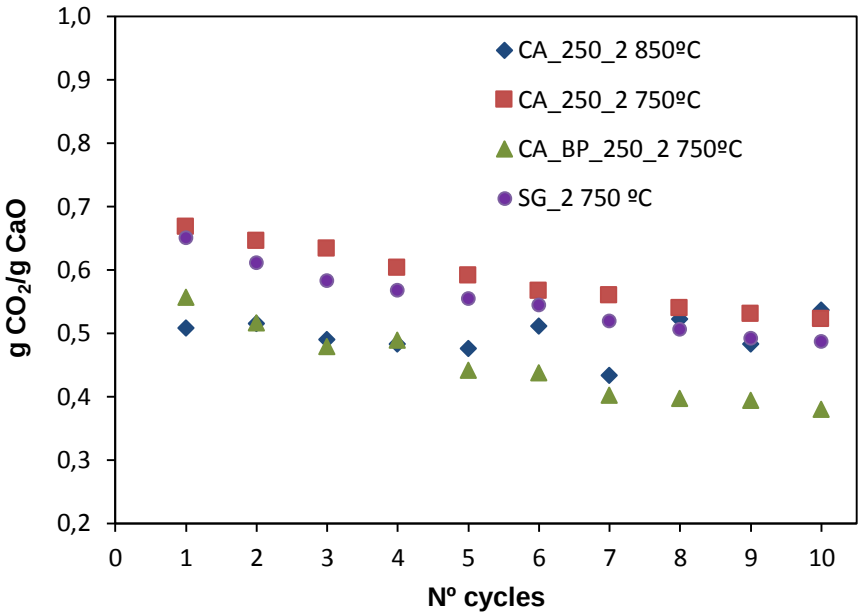

Figure 55: Influence of calcination temperature and type of structurant in CaO-sorbents

The sorbent CA_250_2 750ºC prepared with granular activated carbon and calcined at 750ºC in the preparation step, present a higher initial activity (66.7%) when compared with the samples calcined at 850ºC (50.7%). However, this sorbent CA_250_2 850ºC shows a constant activity and good stability and does not deactivate along the 10 cycles, while the activity of sorbent CA_250_2 calcined at 750ºC decreases 1.6% throughout the 10 cycles until achieving the same carrying capacity of sorbent CA_250_2 850ºC on the 10th carbonation cycle. Since calcination of the activated carbon is a highly exothermic process, the heat released during the calcination at the end of the sorbent preparation will cause a local temperature increase producing a sintering effect in the solid sorbent, which will be stronger in the case of the higher calcination temperature of 850 ºC used in the preparation of the sorbent CA_250_2 850ºC (20). For this reason, for lower calcination temperatures the initial sorbent activity for CO_2 capture is higher as for the case of the sorbent CA_250_2 750ºC prepared in this work.

Comparing both structurants used in this work, granular activated carbon resulted better than carbon BP2000. Both sorbents CA_250_2 750ºC and CA_BP_250_2 750ºC were calcined at 750 ºC for doing the comparison at the same preparation conditions. The sorbent prepared with activated carbon shows a higher initial activity than the sorbent prepared with carbon BP2000, but both have the same deactivating tendency for the rate of activity decay along the 10 cycles.

When comparing the results obtained for sorbent SG_2 750ºC prepared without structurant and calcined at 750 ºC, with sorbent CA_250_2 750ºC prepared with structurant granular activated carbon calcined at the same temperature of 750 ºC (Fig. 55) it is possible to see that sorbent CA_250_2 750ºC has a slightly higher initial CO_2 capture activity and that this sorbent has a smaller rate of deactivation along the 10 cycles although this deactivation rate is not very different from the case of sorbent SG_2 750ºC.

In this section it was not possible to compare the CO_2 capture activity and sorbent stability results obtained for the non-supported synthetic CaO-based sorbents with those for the Ca/SBA-15 sorbents due to the reasons that have been explained in the previous section.

6 CONCLUSIONS

The goal of this work was the synthesis of a stable SBA-15 mesoporous material with the purpose of being used as a support material for Ca-based sorbents used in the calcium-looping cycle CO_2 capture. Microwave-assisted (MW) method was used during the synthesis, in order to study the different advantages compared to the conventional method.

Several samples of SBA-15 were synthesized by conventional and MW method and calcined at different temperatures, analyzing the thermal stability by different characterization techniques: thermogravimetric analysis (TGA-DSC), X-Ray diffraction (XRD) and nitrogen sorption measurement. Using optimized MW synthesis conditions, a SBA-15 sample was synthesized and used to impregnate calcium nitrate in order to obtain suitable sorbents for CO_2 capture evaluation.

The most important difference between conventional and MW synthesis methods was that the later allows to program and control easily temperature and time during synthesis and reduces the hydrothermal treatment duration from days to hours, without sacrificing the quality of the final porous materials. MW-assisted method allowed to obtain a SBA-15 material with higher thermal stability than the one prepared under conventional method, even calcined at 900ºC maintaining the ordered mesoporous structure, thus being suitable as support of CaO particles. High temperatures (170ºC) and 2 hours of crystallization under MW were determined as optimal conditions to synthesis a SBA-15 material presenting a high hexagonal ordered.

10 and 20 wt.-%Ca impregnated samples were tested in the lab-scale CO_2 capture unit but due to the very small amount of Ca impregnated the consequent amount of CO_2 captured was not detected by the CO_2 detector. However, the ordered mesoporous structure was maintained after Ca impregnation and even after the Ca/SBA-15 mesoporous sorbents were tested in the lab-scale CO_2 capture unit. The tests performed in the TG unit were effective, showing low reactivity values for both sorbents, thus confirming the necessity to use Ca/SBA-15 sorbents with high Ca loading.

Three synthetic non-supported CaO sorbents were also synthesized and studied in this work for a better understanding of the influence of using a structurant in the sol-gel preparation step (granular activated carbon AC and carbon BP2000), of the influence of the calcination temperature at the end of the sol-gel preparation step, and also for comparing their CO_2 capture activity with that of the prepared Ca/SBA-15 supported sorbents.

The results showed a higher initial CO_2 adsorption capacity of the sorbent prepared with AC and calcined at 750 ºC, being also higher than the initial CO_2 adsorption capacity obtained with structurant carbon BP2000, probably due to the larger size of the granular activated carbon particles which create larger pores during carbon burning. However, both have the same deactivating tendency for the rate of activity decay along the 10 cycles. When comparing the results obtained for the non-supported sorbent prepared without structurant and calcined at 750 ºC, with the sorbent prepared with AC and calcined at the same, it is possible to conclude that sorbent prepared with AC has a slightly higher initial CO_2 capture activity and that this sorbent has a smaller rate of deactivation along the 10

cycles although this deactivation rate is not very different from the case of the sorbent prepared without structurant.

The results obtained for the CO_2 capture activity with the sorbents prepared with AC and calcined at 750 and 850ºC, showed that the calcination temperature at the end of the sol-gel preparation step is an important parameter. Since AC calcination is a highly exothermic process, the heat released during the calcination will cause a local temperature increase producing a sintering effect in the solid sorbent, which will be stronger at 850 ºC. For this reason, for lower calcination temperatures the initial sorbent activity for CO_2 capture is higher as for the case of the sorbent prepared with AC and calcined at 750ºC.

Comparisons with the reactivity of Ca/SBA-15 sorbents could not be made due to the experimental limitations explained earlier.

FUTURE WORK

As future work, impregnation of higher amounts of Ca in the SBA-15 mesoporous supports could be studied, in order to test the effectiveness of CaO-based SBA-15 sorbents in the CO_2 capture process. The following amounts (40, 50 and 60 wt.-% of calcium with respect to SBA-15 support) could be tested. It would be also necessary to carry out the corresponding characterizations of the impregnated samples: TG-DSC, XRD, N_2 sorption and SEM. It could be also interesting to use other Ca sources or even other impregnation methods and evaluate their effect on the final CO_2 capacity properties.

Another interesting topic that could be also studied more in depth concerns the influence of the calcination temperature of the CaO-samples prepared by the sol-gel method with respect to material reactivity in CO_2 adsorption. In addition, new synthetic sorbents could be prepared using nano-cellulose as structurant and compared with the results obtained with activated carbon structurant.

REFERENCES

[1]. **United States Environmental Protection Agency (EPA)**. [Consulted on: 3 May of 2014] http://www.epa.gov/climatechange/ghgemissions/global.html.

[2]. Olajire, Abass A. ***CO_2 capture and separation technologies for end-of-pipe applications***. Elsevier, 2010.

[3]. D'Alessandro, Deanna M.; Smith, Berend; Long, Jefrrey R. ***Carbon Dioxide Capture: Prospects for New Materials.*** Angewandte Chemie International Edition, 2010.

[4]. Blamey, J.; Anthony, E.J.; Wang, J.; Fennell, P.S. ***The calcium looping cycle for large-scale CO2 capture.*** Elsevier, 2009.

[5]. **European Environmental Agency (EEA)**. [Consulted on: 3 May of 2014] http://www.eea.europa.eu/data-and-maps/indicators/greenhouse-gas-emission-trends/greenhouse-gas-emission-trends-assessment-5.

[6]. **Center for Climate and Energy Solutions (C2ES)**. [Consulted on: 3 May of 2014] http://www.c2es.org/facts-figures/international-emissions/historical.

[7]. Markusson, N.; Kern, F.; Watson, J.; Arapostathis, S.; Chalmers, H.; Ghaleigh, N.; Heptonstall, P.; Pearson, P.; Rossati, D.; Russell, S. ***A socio-technical framework for assessing the viability of carbon capture and storage technology***. Elsevier, 2011.

[8]. Bowen, F. ***Carbon capture and storage as a corporate technology strategy challenge.*** Elsevier, 2011.

[9]. Wang, S.; Yan, S.; Ma, X.; Gong, J. ***Recent advances in capture of carbon dioxide using alkali-metal-based oxides.*** Science, Energy & Environmental, 2011.

[10]. Huang, C.H.; Chang, K.P.; Yu, C.T.; Chiang, P.C.; Wang, C.F. ***Development of high-temperature CO2 sorbents made of CaO-based mesoporous silica.*** Elsevier, 2010.

[11]. Dean, C.C.; Blamey, J.; Florin, N.H.; Al-Jeboori, M.J.; Fennell, P.S. ***The calcium looping cycle for CO2 capture from power generation, cement manufacture and hydrogen production.*** Elsevier, 2011.

[12]. Santos, E.T.; Alfonsín, C.; Chambel, A.J.S.; Fernandes, A.; Soares Dias, A.P.; Pinheiro, C.I.C, Ribeiro, M.F. ***Investigation of a stable synthetic sol–gel CaO sorbent for CO2 capture.*** Elsevier, 2011.

[13]. **Community Research and Development Information Service.** European Commission. [Consulted on: 10 May of 2014] http://cordis.europa.eu/result/report/rcn/59284_en.html.

[14]. Arias, B.; Diego, M.E.; Abanades, J.C.; Lorenzo, M.; Diaz, L.; Martinez, D.; Alvarez, J.; Sanchez-Diezma, A. ***Demonstration of steady state CO2 capture in a 1.7 MWth calcium looping pilot.*** Elsevier, 2013.

[15]. Ströhle, J.; Junk, M.; Kremer, J.; Galloy, A.; Epple, B. ***Carbonate looping experiments in a 1 MWth pilot plant and model validation.*** Elsevier, 2013.

[16]. Nicholas H., F.; Blamey, J.; Fennell, Paul S. ***Synthetic CaO-based sorbent for CO_2 capture from large-point sources.*** Energy&fuels, 2010.

[17]. Sun, P.; Grace, J.R.; Lim, C.J. ***The effect of CaO sintering on cyclic CO_2 capture in energy systems.*** Interscience, 2007.

[18]. Chen, C.; Yang, S.T.; Ahn, W.S. ***Calcium oxide as high temperature CO_2 sorbent: effect of textural properties.*** Elsevier, 2012.

[19]. Abanades, J.C. **Calcium lloping for CO_2 capture in combustion systems.** Spanish Research Council (CSIC), 2013.

[20]. Fernandes Hipólito, Joana. ***Influência das condições operatórias na síntese de adsorventes à base de CaO com carvão ativado na Captura de CO_2.*** Universidade Nova de Lisboa, 2014.

[21]. Florin, N.H.; Fennell, P.S. ***Synthetic CaO-based Sorbent for CO2 Capture.*** Elsevier, 2011.

[22]. Xu, P.; Xie, M.; Cheng, Z.; Zhou, Z. ***CO2 Capture Performance of CaO-Based Sorbents Prepared by a Sol−Gel Method.*** I&EC Research, 2013.

[23]. Norhasyimi, R.; Abdullah, A.Z.; Mohamed, A.R. ***A review: mesoporous Santa Barbara Amorphous-15, types, synthesis and its applications towards biorefinery production.*** *American Journal for Applied Sciences* 2010.

[24]. Zhao, D.; Fenq, J.; Huo, Q.; Melosh, N.; Fredrickson, G.H.; Chmelka, B.F.; Stucky, G.D. ***Triblock Copolymer Syntheses of Mesoporous Silica with Periodic 50 to 300 Angstrom Pores.*** SCIENCE, 1998.

[25]. Pal N.; Bhaumik, A. ***Soft templating strategies for the synthesis of mesoporous materials: inorganic, organic-inorganic hybrid and purely organic solids.*** Elsevier, 2013.

[26]. Han, S.C.; Jiang, N.; Burri, S.D.; Choi, K.M.; Lee, S.C.; Park, S.E. ***Microwave synthesis of SBA-15 mesoporous silica material for beneficial effect on the hydrothermal stability.*** Elsevier, 2007.

[27]. Celer, E.; Jaroniec, M. ***Temperature-Programmed Microwave-Assisted Synthesis of SBA-15 Ordered Mesoporous Silica.*** 2006.

[28]. Benamor, T.; Vidal,L.; Lebeau, B.; Marichal, C. ***Influence of synthesis parameters on the physico-chemical characteristics of SBA-15 type ordered mesoporous silica.*** Elsevier, 2011.

[29]. Zhao, D.; Huo, Q.; Feng, J.; Chmelka, B.F.; Stucky, G.D. ***Nonionic Triblock and Star Diblock Copolymer and Oligomeric Surfactant Syntheses of Highly Ordered, Hydrothermally Stable, Mesoporous Silica Structures.*** American Chemical Society, 1998.

[30]. International Equipment Traiding (IET). ***Mars5 Data Sheet.***

[31]. CEM corporation. ***Operation Manual: Microwave Accelerated Reaction System.*** 2001.

[32]. CABOT Norit ACtivated Carbon. [Consulted on: 25 June of 2014] http://www.norit.com/products-and-services/products/norit-gac-1240-plus/.

[33]. Sun, H.; Han, J.; Ding, Y.; Li, W.; Duan, J.; Chen, P.; Lou, H.; Zheng, X. ***One-pot synthesized mesoporous Ca/SBA-15 solid base for transesterification of sunflower oil with methanol.*** Elsevier, 2010.

[34]. Schneider, Petr. ***Adsorption isotherms of microporous-mesoporous solids revisited.*** Elsevier, 1995.

[35]. Lowell, S.; Shields, J.E.; Thomas, M.A.; Thommes, M. ***Characterization of porous solids and powders: surface area, pore size and density.*** Kluwer Academic Publishers, 2004.

[36]. Thommes, Matthias. ***Physical Adsorption Characterization of Nanoporous Materials.*** Chemie Ingenieur Technik, 2010.

[37]. **Alfonsín Outeda, Carolina.** *CaO based sorbents looping cycles for CO2 capture.* Instituto Superior Técnico, 2011.